Tectonophysics 609 (2013) 184–201

Contents lists available at ScienceDirect

Tectonophysics

journal homepage: www.elsevier.com/locate/tecto

Review Article

Constraints on the Moho in Japan and Kamchatka

Takaya Iwasaki [a], Vadim Levin [b,*], Alex Nikulin [b], Takashi Iidaka [a]

[a] Earthquake Research Institute, University of Tokyo, Japan
[b] Rutgers University, NJ, USA

ARTICLE INFO

Article history:
Received 1 July 2012
Received in revised form 12 November 2012
Accepted 22 November 2012
Available online 3 December 2012

Keywords:
Kamchatka
Japan
Crustal structure
Upper-mantle structure
Moho

ABSTRACT

This review collects and systematizes in one place a variety of results which offer constraints on the depth and the nature of the Moho beneath the Kamchatka peninsula and the islands of Japan. We also include studies of the Izu–Bonin volcanic arc. All results have already been published separately in a variety of venues, and the primary goal of the present review is to describe them in the same language and in comparable terms. For both regions we include studies using artificial and natural seismic sources, such as refraction and reflection profiling, detection and interpretation of converted-mode body waves (receiver functions), surface wave dispersion studies (in Kamchatka) and tomographic imaging (in Japan). The amount of work done in Japan is significantly larger than in Kamchatka, and resulting constraints on the properties of the crust and the uppermost mantle are more detailed.

Japan and Kamchatka display a number of similarities in their crustal structure, most notably the average crustal thickness in excess of 30 km (typical of continental regions), and the generally gradational nature of the crust–mantle transition where volcanic arcs are presently active.

Contents

* Corresponding author. Fax: +1 445 5312.
E-mail address: vlevin@eps.rutgers.edu (V. Levin).

0040-1951/$ – see front matter © 2012 Elsevier B.V. All rights reserved.
http://dx.doi.org/10.1016/j.tecto.2012.11.023

1. Introduction

The primary purpose of this brief review is to collect, systematize and present in a common format a variety of results which offer constraints on the depth and the nature of the Moho beneath Kamchatka and Japan, which form the eastern margin of the Asian continent. These areas have been studied for decades, with a variety of geophysical methods, including active and passive seismic methods, gravity and other techniques.

The Moho and the upper mantle structures in and around Japan have been well investigated both from active and passive seismic source studies including marine expeditions. Earlier results on these subjects (1960–1970s) were mainly presented from seismic refraction experiments (Yoshii, 1994). The advance of technology in data acquisition and processing systems in 1980 and 1990s brought us a large amount of high quality seismic data (Yoshii, 1994; Iwasaki et al., 2002). In active source experiments, the receiver spacing became much denser (less than 2–3 km), which enabled us to identify many seismic phases including reflections from the Moho (PmP phase) and improve the constraints on the nature of the Moho boundary. After the 1995 Kobe earthquake, a new and denser seismic network has been established in Japan. It was subsequently used to carry out detailed tomography analyses and receiver function investigations that provided constraints on the lateral variations in Moho geometry and the uppermost mantle velocity beneath Japan.

Due to the strategic importance of Kamchatka during the Cold War, and the general culture of research publications in the former Soviet Union, many published results on the crustal structure are somewhat cryptic, especially where spatial locations are concerned. In this review we undertook an effort of digitizing and geo-referencing all published results available in the peer-reviewed literature, in both Russian and English languages. No attempt was made to locate local publications or archival copies of technical reports that potentially contain some of the primary data. In other words, we are presenting results as they have been published, and provide only a minimum of commentary.

Hereafter, we present several important features of Moho and upper-mantle structure beneath Japan and Kamchatka from various methodologies that are described in the following section. For each region we present, in turn, a brief overview of relevant tectonic features, and subsequently describe specific constraints on the Moho. We conclude this review with a discussion of similarities and differences between these two regions.

2. Summary of methods

2.1. Compressional wave refraction and reflection

The primary method for detecting the crust–mantle boundary relies on observations of refracted compressional waves. This technique is commonly employed with artificial sources (blasts on land or air guns at sea), and a common practice is to interpret both refracted and post-critically reflected waves, identified on record sections on the basis of their apparent velocities. A version of the method commonly used in the USSR during the second part of the XX century was referred to as the Deep Seismic Sounding (DSS) technique. After 1980–1990s, ray tracing technique became a standard tool for seismic refraction/wide-angle reflection profiling. By combining travel time and amplitude data, we could obtain detailed structure of the deeper part of crust and upper-mantle. Near-vertical reflection profiling is quite an effective tool to image crust and upper-mantle structure particularly in the continents. In Kamchatka or Japan, however, it is quite rare to obtain clear image around the Moho boundary due to high seismic attenuation arising from their complex structures and intense volcanic activities.

2.2. Mode conversion in body waves

Records of compressional seismic waves from distant earthquakes typically contain both compressional- and shear-polarized waves within their coda. The shear-polarized phases are understood to arise from mode conversions between compressional and shear waves that take place when compressional waves encounter sharp gradients in seismic impedance (density–velocity product) (Phinney, 1964; Vinnik, 1977). The Moho is expected to give rise to a prominent P-to-S converted phase. Recognition of this phase, and timing of its arrival with respect to the "parent" compressional wave, offers a constraint on the depth to the converting boundary (e.g., Langston, 1981). Frequency, amplitude and signature of the waveform associated with the Moho P-to-S converted wave can be used to assess the nature of the boundary (e.g. vertical extent of the gradient in impedance). A "receiver function" technique (e.g., Ammon, 1991) relies on the similarity in waveform shapes of parent P and daughter S waves, and employs time-series manipulation algorithms to isolate the latter in digital records of teleseismic P waves. Results of such processing are records of shear waves in "relative time" that may be interpreted as a proxy for the depth to a converting interface. A common practice is to combine multiple observations, and to explore the changes in timing and appearance of converted phases with respect to direction of propagation (back azimuth and angle of incidence), making sure that the phase being interpreted is indeed a direct P-to-S converted wave. The timing of converted phases is subject to a trade-off between the depth of the converting interface and the ratio of P and S wave speeds (e.g. Gurrola et al., 1995).

2.3. Surface waves

In a layered medium with depth-variable seismic properties surface waves propagate with the speed dependent on their period. Waves with progressively longer periods (and consequently larger wavelengths) sample progressively deeper parts of the Earth. A resulting relationship of speed vs period (known as a "dispersion relationship") can be interpreted in terms of the vertical distribution of speed. Key assumptions that are involved in this approach are a) that the medium is horizontally stratified and b) the properties change only vertically in the volume enclosing both the source and the receiver. A common strategy is to divide the region of study into areas containing distinct source–receiver paths, and to develop independent velocity–depth profiles for them. In this approach, the depth to the Moho can be estimated, either as a depth of a strong gradient in speed or, alternatively, a depth where the speed reaches a value characteristic of the upper mantle rock.

2.4. Tomographic imaging

Constraints on the depth to the crust–mantle boundary may be obtained in conjunction with detailed tomographic imaging of the lithosphere on the basis of regional body wave observations. While tomography commonly starts with an a priori vertical profile of seismic wave speed, depths of major velocity contrasts may be included in the model part of the inverse problem. Alternatively, tomographically imaged velocity anomalies may suggest the need to move pre-determined boundaries in velocity.

2.5. Observations of gravity field strength

In accordance with the principle of Airy isostacy, an excess of topographic elevation should be compensated with extra thickness of the crust, and vice versa. Consequently, observations of gravity field anomalies may be converted into crustal thickness after corrections for known topography are taken into account. The conversion assumes known densities at depth, as well as the thickness of the reference crust at sea level that yields no anomaly.

3. Moho investigations in Japan

3.1. Tectonic setting in and around Japan

The Japanese islands are situated along subduction zones along the eastern margin of the Asian continent (Fig. 1). They have developed under complex tectonic processes dominated by plate subduction, accretion, backarc spreading and arc–arc collision. Major islands of Hokkaido, Honshu, Shikoku and Kyushu are geologically divided into two arcs of NE Japan and SW Japan. The NE Japan Arc includes northern Honshu and western Hokkaido. The Pacific Plate is being subducted with a velocity of 8 cm/y to WNW direction beneath the NE Japan Arc. The SW Japan Arc consists of the western half of Honshu, Shikoku and Kyushu, beneath which the Philippine Sea Plate is subducted to WNW direction with a rate of 3–5 cm/y. During most of the Mesozoic to early Miocene time, these arcs were situated along the subduction zone in the eastern margin of the Asian continent, and rotated to their present locations by backarc opening of the Sea of Japan in a period of 20–14 Ma (e.g. Otofuji et al., 1985). The extensional stress regime at the time of the backarc opening was changed into compressional stress at 4 Ma in NE Japan and at the beginning of the Quaternary time in SW Japan (e.g. Hujita, 1980; Okamura,

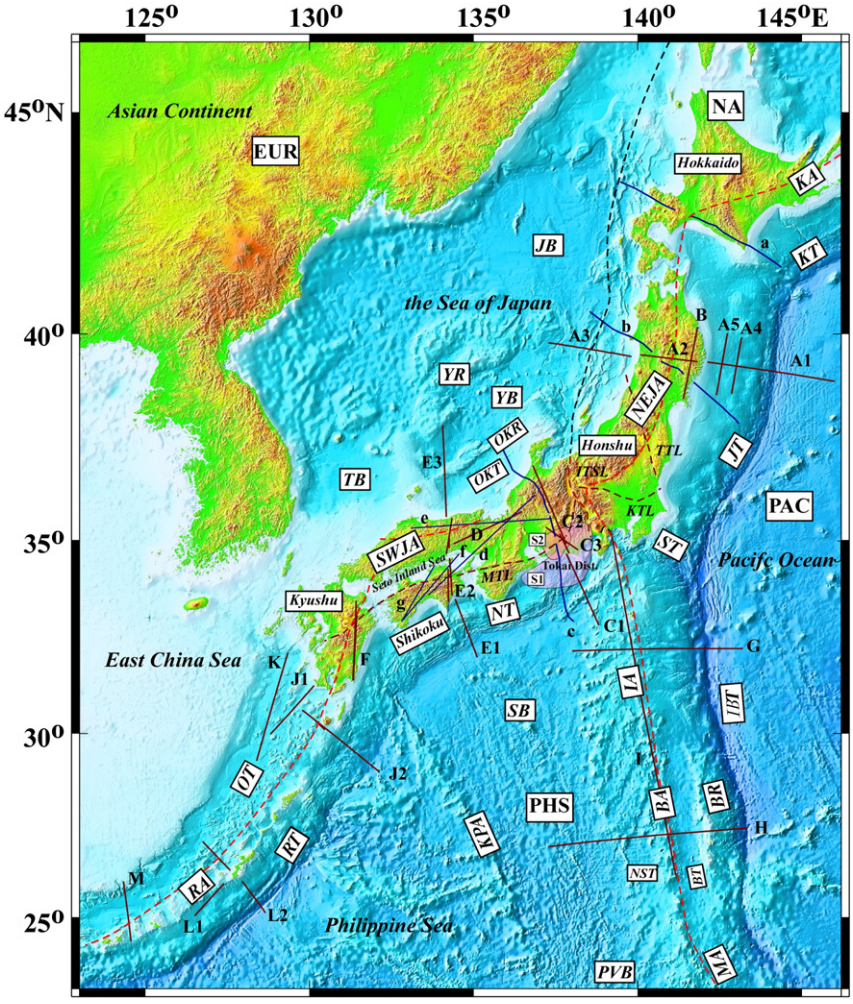

Fig. 1. Tectonic map in and around Japan. EUR: Eurasia Plate. PAC: Pacific Plate. PHS: Philippine Sea Plate. NA: North America Plate. KT: Kuril Trench. KA: Kuril Arc. JT: Japan Trench. NEJA: NE Japan Arc. ST: Sagami Trough. NT: Nankai Trough. SWJA: SW Japan Arc. IBT: Izu–Bonin Trench. IA: Izu Arc. BR: Bonin Ridge. BA: Bonin Arc. KPR: Kyushu–Palau Ridge. MA: Mariana Arc. PVB: Parece-Vela Basin. RT: Ryukyu Trench. RA: Ryukyu Arc. OT: Okinawa Trough. JB: Japan Basin. YB: Yamato Basin. YR: Yamato Ridge. OKT: Oki Trough. OKR: Oki Ridge. TB: Tsushima Basin. SB: Shikoku Basin. BT: Bonin Trough. NST: Nishinoshima Trough. Quaternary volcanic front is indicated by a red dash line. Brown dash lines show major tectonic lines. ISTL: Itoigawa–Shizuoka Tectonic line. TTL: Tanagura Tectonic line. KTL: Kanto Tectonic Line. MTL: Median Tectonic Line. S1: Source area expected for the forthcoming Tokai earthquake (e.g. Ando, 1975; Mogi, 1981). S2: A slow slip area in the Tokai District (Ozawa et al., 2002). Major seismic lines are also shown. Blue lines are earlier profiles (1960–1970s). Recent profiles are indicated by brown lines.

1990; Sato, 1994). Nakamura (1983) pointed out that new subduction initiated at 1–2 Ma west of the NE Japan. This means that the northern part of Japan belongs to the North American Plate (Fig. 1). This issue, however, is still controversial due to geological/geophysical observations indicating that the former subduction zone in the central part of Hokkaido is active (e.g. Iwasaki et al., 2004; Kazuka et al., 2002; Sato and Ikeda, 1994).

There exist several major tectonic lines within the NE Japan and SW Japan Arcs. The Itoigawa–Shizuoka Tectonic Line (ISTL), running with NS direction in Central Japan, is a major tectonic boundary and one of the most active fault systems. According to Nakamura (1983), the plate boundary in the Sea of Japan is connected with the ISTL, separating the North American Plate from Eurasia (Amur) plate. The Kanto Tectonic Line (KTL) is considered to separate the SW Japan Arc from the NE Japan Arc. A syntaxis by the ISTL and KTL has been formed by the collision of the Izu–Bonin–Mariana (IBM) Arc against the SW Japan Arc since the middle Miocene. The Median Tectonic Line (MTL) is the most prominent active fault with EW strike in SW Japan, dividing the SW Japan Arc into the Inner (northern side) and the Outer (southern side) Zones (e.g. Ito et al., 2009; Yamakita and Otoh, 2000). The Outer Zone is composed of Jurassic–Miocene accretionary complexes, whose northernmost part was affected by high P/T metamorphism (the Sambagawa Belt). The Inner Zone consists of geological units with older ages (180–2000 Ma) (Isozaki and Maruyama, 1991), a part of which experienced heavy granitic intrusion at the time of Cretaceous.

From the central to eastern parts of Hokkaido, another arc–arc collision zone is ongoing. Since Miocene, the Kuril Forearc, now occupying the southernmost part of eastern Hokkaido, has been collided against the western Hokkaido (the NE Japan Arc).

Off the southern part of central Honshu, the Japan Trench, Sagami Trough and Izu–Bonin Trough meet together forming a triple junction to produce complex structures. The Izu–Bonin–Mariana (IBM) Arc, 2800 km in length, has been formed in an intraoceanic convergent margin in contrast with the NE Japan and SW Japan Arcs built on the continental crust. The initial subduction along the Izu–Bonin and Mariana Trenches started at 50–40 Ma (~43 Ma), forming a proto-type IBM Arc (e.g. Stern et al., 2003). By the first rifting occurring in 30–15 Ma, the Kyushu–Palau Ridge was separated to the west to open the Parece–Vela and Shikoku Basins. The northernmost part of the Izu Arc began to collide against Honshu by the initiation of subduction along the Nankai Trough at 15 Ma. The second rifting started after 10 Ma in the southern part of the IBM Arc, which is responsible to form the Mariana-back arc basin. The northern Izu Arc, on the other hand, has evolved as an unrifted arc.

The Ryukyu Arc, extending from Kyushu to Taiwan, consists of a nonvolcanic outer arc and a volcanic arc (e.g. Sibuet et al., 1987). Behind the Ryukyu Arc, there exists a backarc basin of the Okinawa Trough. The initiation of rifting of this basin is dated late Miocene (Letouzey and Kimura, 1985) or early Pleiocene (Park et al., 1998). It is considered that the middle and southern Okinawa Trough is in a more advanced stage of backarc spreading than further north (e.g. Sibuet et al., 1987). Namely, the backarc spreading phase started very recently in the southern Okinawa Trough, while the northern Okinawa Trough is in a stage of the crustal thinning.

Seismic activity is extremely high in and around the NE Japan and SW Japan Arcs, as characterized by M8–9 class interplate earthquakes along the Japan Trench, Sagami Trough and Nankai Trough. Furthermore, M7 class intraplate earthquakes occurring in inland areas. Recent microseismic observations revealed that most of the crustal earthquakes are concentrated in a depth range of 0–15 km, which shows a marked contrast with a very low seismic activity in the lower crust (Ito, 1993, 1999). Deeper events in the NE Japan are concentrated within the subducting Pacific Plate down to 200 km (e.g. Hasegawa et al., 1978; Kita et al., 2010). In the SW Japan, such seismic planes within the PHS plate are less developed and limited at a depth shallower than 60 km (e.g. Ishida, 1992; Okano et al., 1985).

3.2. Overview of earlier refraction/wide-angle reflection studies in 1960–1970s

First constraints on Moho and upper-mantle velocity were obtained from seismic refraction studies in 1960–1970s by the Research Group for Explosion Seismology, Japan (RGES). Very early results were reviewed by RGES (1966), showing the upper-mantle velocity and Moho depth are 7.5–8.0 km/s and 20–38 km, respectively. The best known crustal and upper-mantle section in this period was obtained for Profile b crossing NE Japan (Figs. 1 and 2) from a series of seismic experiments (Asano et al., 1979; Okada et al., 1979; Yoshii and Asano, 1972; Yoshii et al., 1981). The most important feature of this model is an anomalously low Pn velocity (~7.5 km/s) beneath the NE Japan Arc. The crust of the NE Japan Arc is 30 km thick, composed of upper and lower layers with a velocity of 5.9 and 6.6 km/s, respectively. Another important aspect of this section was the Moho depth variation for both the fore-arc and the back-arc regions. Remarkable crustal thinning, with the crust being reduced to 17–18 km in thickness, was seen as related to the Miocene opening of the Sea of Japan. The Pn velocity in this part is 8 km/s, much higher than that beneath the arc. Also, the Pn velocity beneath the fore-arc of the NE Japan Arc is almost 8 km/s (Asano et al., 1981; Okada et al., 1979; Yoshii et al., 1981). Hence, it is said that the low Pn velocity of 7.5 km/s is a characteristic of the NE Japan Arc. Actually, almost the same Pn velocity is reported in southwestern Hokkaido (Profile a in Fig. 1), which geologically belongs to the NE Japan Arc (Okada et al., 1973).

In the SW Japan Arc, slightly higher Pn velocity (7.6–7.8 km/s) is obtained from Profile c (Aoki et al., 1972), Profile d (Aoki and Muramatsu, 1974), Profile e (Yoshii et al., 1974), Profile f (Ikami et al., 1982) and Profile g (Ito et al., 1982) in Fig. 1. The Moho depth from these profiles is in the 30–40 km range. Generally, resolution for crustal structures in the earlier results was relatively low due to limitations of experimental design (sparse spacing of shots (100–200 km) and receivers (5–10 km)), which resulted in considerable ambiguity in Moho depth estimation. However, compared with cases of continental or oceanic uppermost mantle it is clear that the uppermost mantle velocity beneath the Japanese islands directly determined from the first arrivals of Pn phase is low (less than 8.0 km/s).

3.3. Crust and upper-mantle sections from recent active-source seismic experiments

3.3.1. The NE Japan Arc

An onshore–offshore wide-angle seismic experiment in 1997 (Profiles A1–3) provided a new and detailed crustal section across the NE Japan Arc (Nishisaka et al., 1999, 2001; Iwasaki et al., 2001; Takahashi et al., 2004; Fig. 3). The improvement of experimental technology enabled much denser shot and receiver spacing (5–30 km and 500 m, respectively) as compared with the earlier cases in Section 3.2. The eastern part of the onshore part (Profile A2, Iwasaki et al., 2001) has been a stable fore-arc block during the Miocene backarc spreading, which is composed of a less deformed upper/middle crust of higher velocity (6.0–6.05–6.3 km/s) with a number of reflectors below a depth of 10–12 km. The total crustal thickness of this block is 32–33 km. Similar structural features are found for Profile B (Iwasaki et al., 1994) running in NS direction in the fore-arc part. The Moho depth beneath this profile is 32–34 km. The western part of Profile A2 is covered with thick Miocene sediments. This package shows complicated geometry, representing extensional basins with Miocene normal faulting. The velocities of upper, middle and lower crusts are 5.75–6.15, 6.15–6.30 and 6.6–7.0 km/s, respectively. The upper and middle crustal velocities are clearly lower than those in the eastern part of the profile. The Moho depth exceeds 35 km near the present volcanic front (see Fig. 1), and remains almost constant at 10–15 km further to the east. This may be explained by the high volcanic activity (magmatic intrusion/

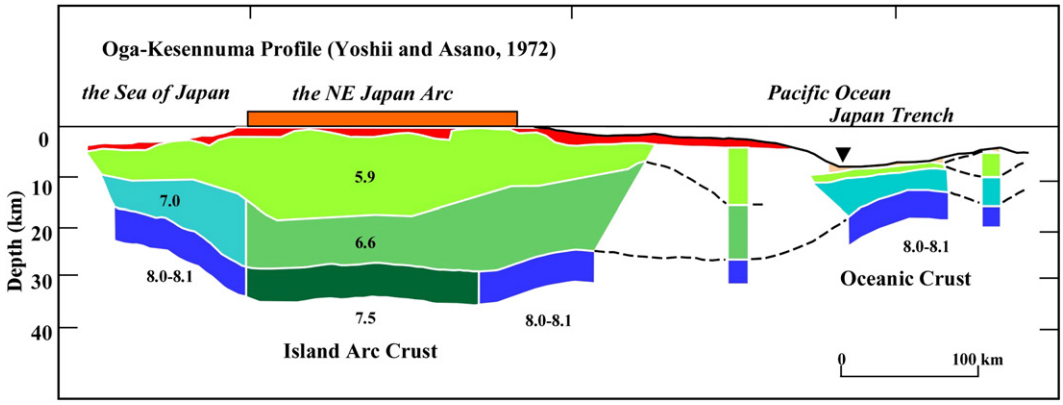

Fig. 2. Early model for crust and upper-mantle structure across the NE Japan reproduced from Iwasaki et al. (2002). Original structure models were presented by Yoshii and Asano (1972) and Okada et al., (1979); (see Profile b in Fig. 1).

underplating) in the last 10–15 Ma (Sato and Amano, 1991). Specifically, the volcanic front prior to 8–10 Ma was situated several tens of kilometers east of the present position. Therefore rather continuous magma supply might have formed the above-mentioned thicker crust. The westward crustal thinning begins at the eastern edge of the Ou backbone range (see "C" in Fig. 3), almost coincident with the eastern limit of the extensional basins, which was also controlled by the crustal stretching during the early Miocene back-arc spreading. While the crust beneath the Yamato Basin shows continental structure (Figs. 1 and 3), the Moho depth there is 18 km, about half the crustal thickness further east (Nishisaka et al., 1999, 2001). It is noted that the thinning is evident in the upper crust, while the lower crust remains constant in thickness. One of the explanations for this is the continuous magmatic underplating west of the Kitakami Lowland. An alternative explanation is that the back-arc spreading progressed in a simple shear mode, allowing the lower crustal thickness to remain unchanged.

As shown in Fig. 3, the lateral variation in Pn velocity is evident across the NE Japan Arc. Ocean bottom seismographic observations in 1990s also support a velocity value of 7.9–8.0 km/s beneath the Sea of Japan (Nishizawa and Asada, 1999; Nishisaka et al., 1999, 2001). Land data from Profile A2, on the other hand, require a low Pn velocity of 7.6–7.7 km/s beneath the western half of NE Japan. These results mean that the Pn velocity change occurs in a 20–30 km wide transition zone beneath the western coast of NE Japan (Iwasaki et al., 2001). Physical explanation of this transition is still enigmatic. Although the thermal regime plays an important role, it cannot sufficiently explain such a sharp transition zone.

Several offshore expeditions (Profiles A4–5) were carried out in the forearc side of the NE Japan (e.g. Miura et al., 2005; Takahashi, et al., 2000, 2004). Below Profile A5, the Moho depth and Pn velocity are obtained as 22 km and 8.0 km/s. This result is consistent to those in the earlier results by Okada et al. (1979), Asano et al. (1981), Yoshii et al. (1981) and Ito et al. (2002).

3.3.2. The SW Japan Arc

Seismic profiling in 1999 and 2002 (Profile E1–3, Kodaira et al., 2002; Kurashimo et al., 2002, 2004; Sato et al., 2006a; Ito et al., 2009) revealed a detailed crustal and upper-mantle section across the western part of the SW Japan Arc (Fig. 4a). The offshore profile (Profile E1, Kodaira et al., 2002) crosses a fault area of 1946 Nankai earthquake (M8.0). One of the important finding from this profile is a subducted seamount which accompanies more than 5 km depression of the oceanic Moho of the PHS plate. Kodaira et al. (2002) investigated the rupture process of the Nankai earthquake and concluded this seamount behaved as a barrier for this event. Further, the upper-mantle velocity beneath the Moho is 7.6 km/s, about 0.2 km/s smaller than that in the surrounding region, indicating intensive serpentinization (Kodaira et al., 2002). The landward increase in Pn velocity is interpreted to be due to the dehydration of the upper-mantle.

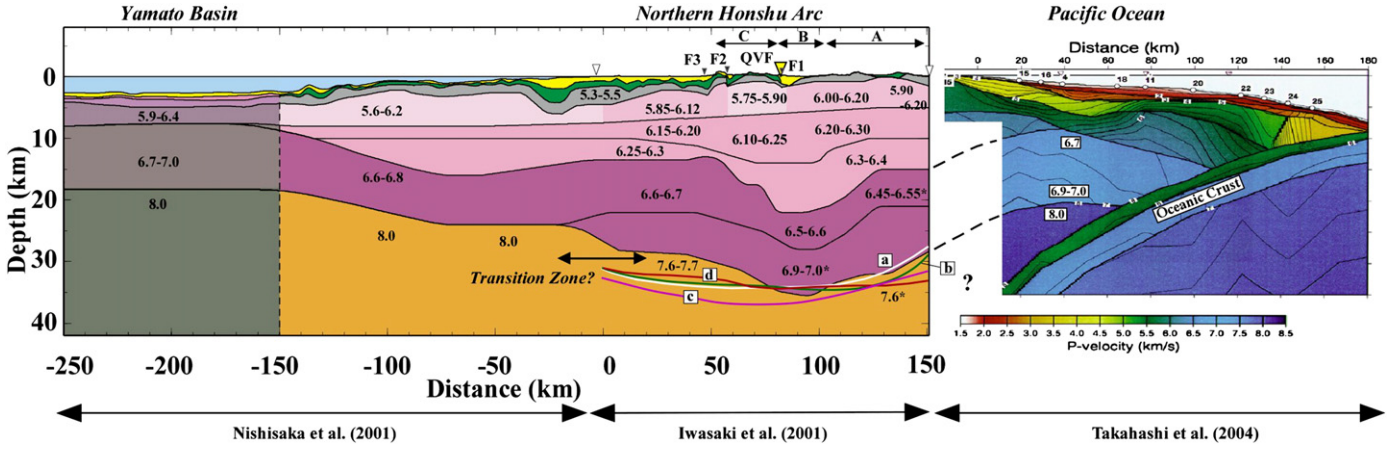

Fig. 3. Crust and upper-mantle section across the NE Japan Arc (Profiles A1–3 in Fig. 1) modified from Iwasaki and Sato (2009). Original structural models were presented by Nishisaka et al. (1999, 2001), Iwasaki et al. (2001) and Takahashi et al. (2004). Open triangles indicate coast lines. A: Kitakami Mountains. B: Kitakami lowland. C: Ou backbone range. F1: Western boundary fault of the Kitakami lowland. F2: Kawafune fault. F3: Sen'ya fault. QVF: Quaternary volcanic front. Crustal thinning is evident in a region from −150 to 0 km. Beneath the Yamato basin (shaded area), the upper and lower crustal thicknesses are almost constant. Lines a–d are Moho depths by Nakajima et al. (2002), Zhao et al. (1990, 1992a) and Katsumata (2010), respectively.

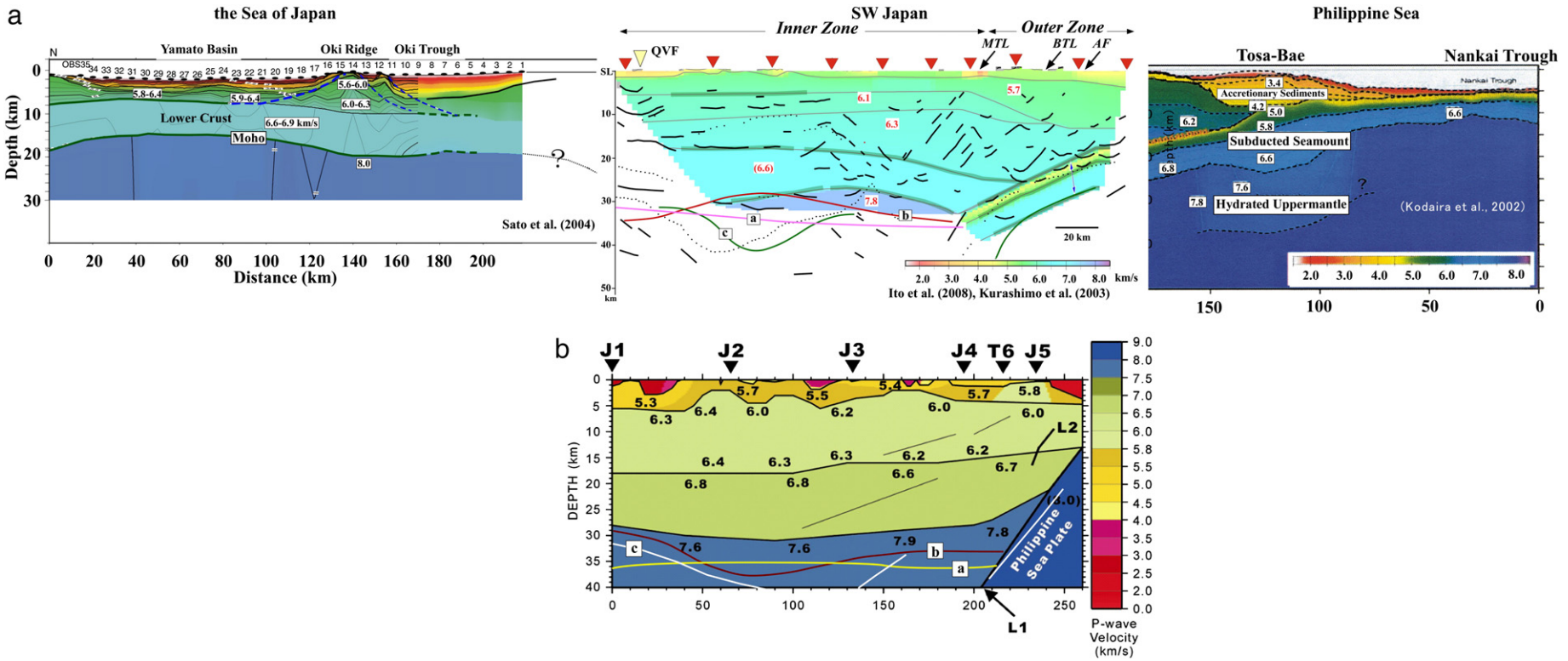

Fig. 4. (a) Crust and upper-mantle section across the western part of the SW Japan Arc (Profiles E1–3 in Fig. 1) modified from Iwasaki and Sato (2009). Original structure models were presented by Kodaira et al. (2002), Kurashimo et al. (2004), Sato et al. (2006a) and Ito et al. (2009). MTL: the Median Tectonic Line. BTL: the Butsuzo Tectonic Line. AF: Aki fault. QVF: Quaternary volcanic front. Lines a–c are Moho depths by Zhao et al. (1992a), Katsumata (2010) and Shiomi et al. (2006), respectively. (b) Crust and upper-mantle section across the eastern part of SW Japan Arc (Profile C2 in Fig. 1) modified from Iidaka et al. (2004). Lines a–c are Moho depths by Zhao et al. (1992a), Katsumata (2010) and Igarashi et al. (2011), respectively.

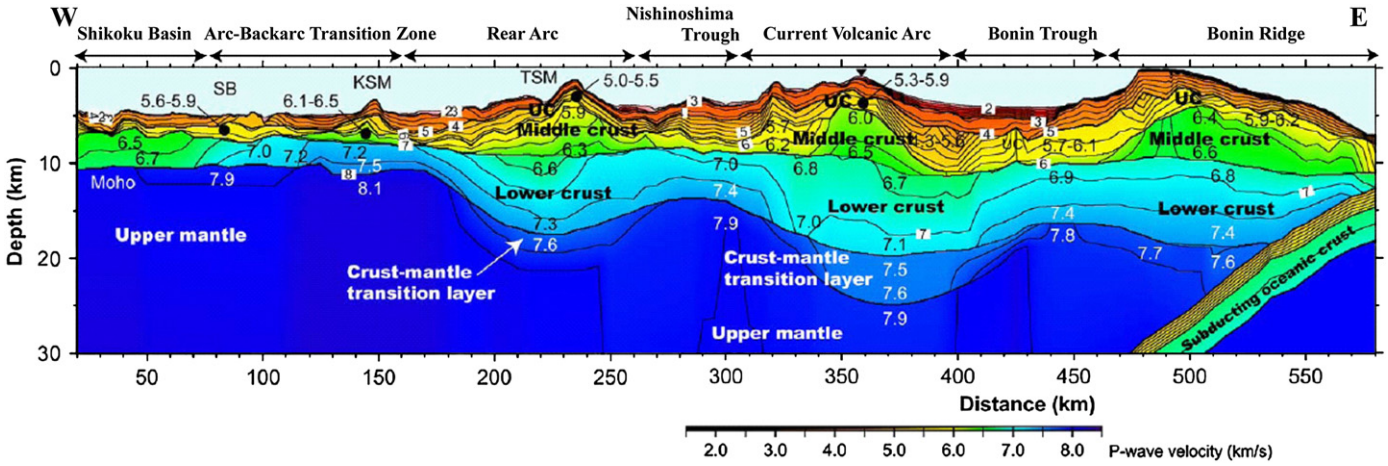

Fig. 5. Crust and upper-mantle section across the southern Izu–Bonin Arc (Profile H in Fig. 1) modified from Takahashi et al. (2009) by permission of American Geophysical Union.

The upper-mantle velocity beneath the SW Japan Arc (Profile E2, Ito et al., 2009; Kurashimo et al., 2002, 2004) is 7.8 km/s, almost consistent with those from the earlier experiments described in Section 3. The Moho depth is 27–30 km, showing concave geometry under the Seto Inland Sea. According to Ito et al. (2009), the MTL cuts the entire crust with a northward dip. It reaches the Moho under the Seto Inland Sea, juxtaposing the two completely different crusts of the Inner and the Outer Zones. Although the crust in the backarc side (Profile E3) shows continental structure, the remarkable crustal thinning is recognized (Sato et al., 2006a). Actually, the crustal thickness is reduced from 30 to 15 km, keeping the lower crustal thickness almost unchanged. This indicates the occurrence of simple shear deformation (Sato et al., 2006a,b), as seen in the backarc side of the NE Japan Arc.

The Moho and upper-mantle structure for Profile C2 was investigated by Iidaka et al. (2004) (Figs. 1 and 4b). In this profile, the Moho is located at a depth of 28–32 km. Pn velocity shows a low value of 7.6 km/s in the northern part of the profile as compared with 7.8–7.9 km in the southern part. The Moho depth in Profile D, running in ENE–WSW direction west of the northern part of Profile C2, is about 35 km with a Pn velocity of 7.6 km/s (Takeda, 2001). So, the upper-mantle velocity may have a large scale variation. Namely, in the southern part of the SW Japan Arc, Pn velocity is around 7.8 km/s, but, approaching to the volcanic front in the northern part, it decreases to 7.6–7.7 km/s.

3.3.3. The Izu–Bonin Arc

The crust and upper-mantle structure in the Izu–Bonin Arc were intensively investigated both from multi-channel reflection and refraction/wide-angle reflection surveys. Structural sections crossing the arc show the remarkable variation in Moho depth from the trench to the backarc side. In the northern part of the Izu–Bonin Arc (Profile G), the crustal thickness is 20 km beneath the central rift zone but reduced to be 8 km beneath the Shikoku Basin (Suyehiro et al., 1996). In the southern part of the Izu–Bonin Arc system (Profile H), Takahashi et al. (2009) showed the crustal thicknesses of the forearc (the Ogasawara (Bonin) ridge), the current volcanic arc and the backarc to be 18, 25 and 16 km, respectively (Fig. 5). The Moho depth decreases towards both sides of the arc where the effect of the rifting is significant. Actually, the crust is reduced in thickness by 50–60%. In contrast with the cases of the NE Japan and SW Japan Arcs, the lower crust with a velocity of 6.6–7.5 km/s is responsible for this thinning. The other important feature is a relatively low velocity (7.5–7.6 km/s) layer situated just above the upper mantle of the current volcanic arc or backarc. Takahashi et al. (2009) interpreted this structure to be the crust–mantle transition zone formed by the accumulation of dense materials emanating from the crust through the crustal growth.

An along-strike structure of the Izu–Bonin Arc is presented by Kodaira et al. (2007). The crust attains its maximum thickness of 32 km in the northern Izu Arc, while a minimum value of ~10 km in the middle of the Bonin Arc. The other feature is undulation of crustal thickness with a scale of ~50 km, well correlated with the locations of basaltic volcanoes along the arc. The responsible factor for this undulation is the middle crust with felsic to intermediate composition created beneath the individual volcano. Kodaira et al. (2007) pointed out that the composition of the middle crust is almost identical to the continental crust. Based on this result, they proposed a scenario for the formation process of continental crust from island arc crust that involves an accumulation of felsic middle crustal materials and delamination of more mafic lower crustal materials.

3.3.4. The Okinawa Trough and Ryukyu Arc

The crust and upper-mantle structure in the Okinawa Trough was intensively investigated in 1980 and 1990s by seismic refraction/wide-angle reflection surveys using ocean bottom seismometers (e.g. Hirata et al., 1990; Iwasaki et al., 1990; Kodaira et al., 1996; Nakahigashi et al., 2004). In the northern part of the trough (Profile J1, Iwasaki et al., 1990), the crust beneath deformed sediments consists of 5.8–6.2 and 6.6–6.9 km/s layers. The Pn velocity is estimated to be less than 7.6 km/s. The Moho depth shows southwestward decrease from 27–30 to 23–24 km. This decrease is mainly due to the upper crustal deformation. The lower crustal thickness is almost constant (13–15 km) along the profile. The crustal structure for Profile K is quite similar to that for Profile J1 (Nakahigashi et al., 2004). The Moho is located at a depth of 27 km at the northern part of the profile, showing slight southward decrease to 25 km. The Pn velocity was obtained as 7.7–7.8 km/s, slightly higher than that for Profile J1 (Iwasaki et al., 1990). Therefore, we can say that the crust in the northern Okinawa Trough is in a stage of thinning associated with the backarc spreading. The oceanic lithosphere subducted beneath the Northern Ryukyu Arc (Profile J2) is traced down to a depth of about 20 km (Iwasaki et al., 1990). The Pn velocity beneath the oceanic Moho is slightly less than 8 km/s. In the middle part of the Ryukyu Arc (Profile L1), the Moho is situated at a depth of about 25 km (Kodaira et al., 1996). For Profile L2, which is perpendicular to Profile L1, the oceanic Moho of the PHS plate is traced from the oceanic basin to 60 km landward of the trench axis. The Pn velocity beneath the oceanic Moho is 8.0 km/s.

In the southern part of the Okinawa Trough (Profile M), the Moho depth is about 18 km (Hirata et al., 1990). The upper crust beneath this profile is highly deformed especially in the vicinity of the trough axis. It is noted that such deformation is not seen to extend in the lower part of the crust.

The structures mentioned above provide direct evidence for the crustal thinning in the Okinawa Trough. This thinning is mainly caused by the decrease in upper crustal thickness to southwest. So, we find the similarity in deformation style of the back-arc spreading to the cases for the NE Japan and SW Japan Arcs.

3.4. 3-D structure of the Moho and the mantle wedge from seismic tomography and receiver function analysis

After the 1995 Kobe earthquake, a new and denser seismic network has been established by the National Research Institute for Earth Science and Disaster (NIED) (Okada et al., 2004). By combining this network with those already operated by Japan Metrological Agency (JMA) and Japanese universities, tomography and intensive receiver function investigations were undertaken to provide two-dimensional (horizontal) variation of Moho geometry beneath Japan.

A series of tomographic studies by Zhao et al. (1990, 1992a,b, 1994) revealed the Moho depth variation in the NE Japan and SW Japan Arcs. In the NE Japan Arc, their result is characterized by a NS trending region with deep Moho (34–36 km) and a lower Pn velocity (7.5 km), almost parallel to the volcanic front. The Moho becomes shallower toward both the fore-arc and the back-arc sides (~30 km). This feature is consistent with the Moho depth determined using travel times of reflected and converted waves from local earthquakes (Nakajima et al., 2002). Along the profile line (Profile A2) by Iwasaki et al. (2001), the Moho depth curves by Zhao et al. (1990, 1992b) and Nakajima et al. (2002) are shown (Fig. 3). The Moho depth variations by Nakajima et al. (2002) and Zhao et al. (1990) are quite consistent with each other along the entire profile. The difference in Moho depth by Zhao et al. (1990, 1992b) may come from the difference in data set and parameters

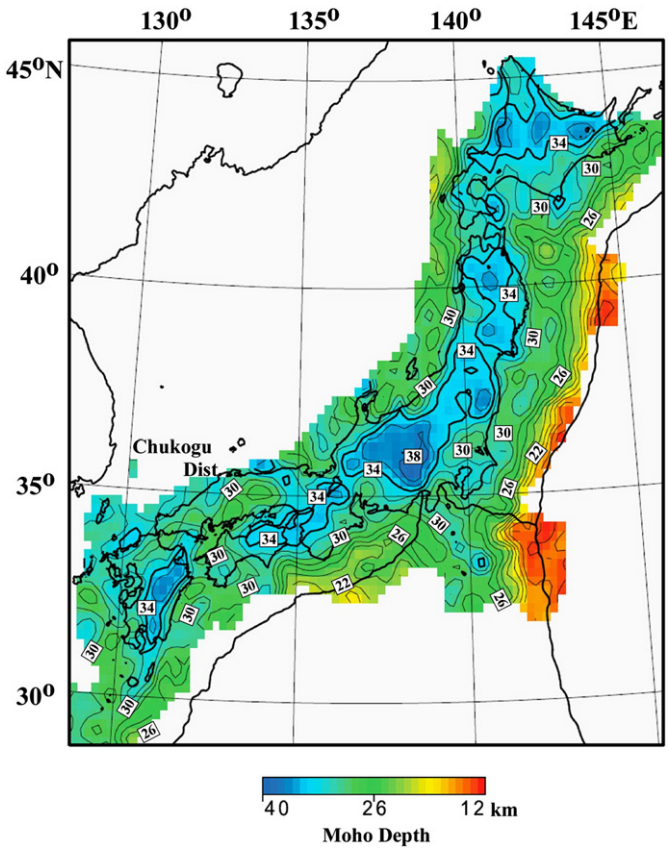

Fig. 6. Moho depth map by tomography analysis modified from Katsumata (2010) by permission of American Geophysical Union. A thick contour line indicates Moho depth of 34 km. Contour interval is 2 km. Moho depth above and below 34 km is shown by red and blue lines, respectively. Contour interval is 1 km.

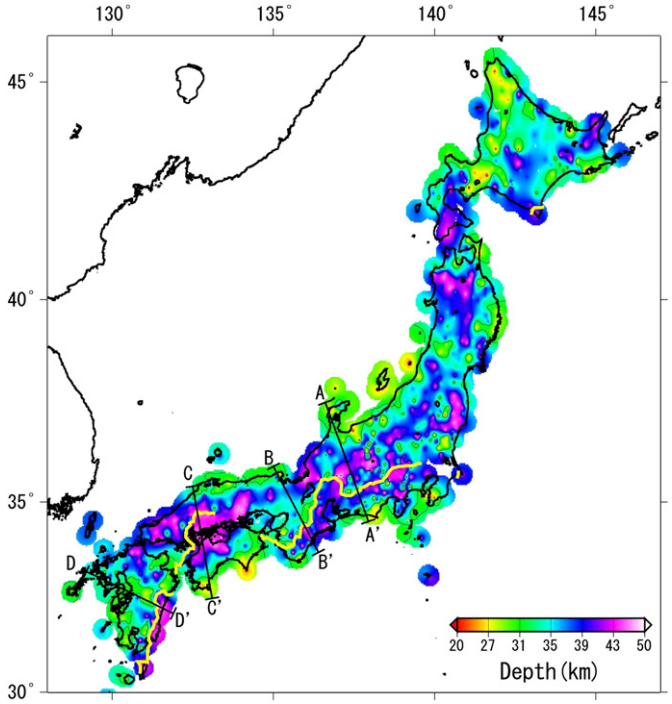

Fig. 7. Moho depth map by receiver function analysis by Igarashi et al. (2011).

used in the inversion analysis. Namely, the former work was focused on the structure beneath the NE Japan (Zhao et al., 1990), while the latter work presented the Moho depth variation beneath the entire part of the NE and SW Japan Arcs (Zhao et al., 1992b). The Moho geometry from these passive seismic source analyses show about 3–7 km discrepancy from the result by Iwasaki et al. (2001) in the western part of the profile. Nakajima et al. (2002) attributed this difference to the lateral structural variation within the crust, which was not taken into account in their analysis. Particularly, the very thick sedimentary package in the extensional basins may yield a significant effect in the Moho depth estimation. Recently, Katsumata (2010) determined the Moho depth map in Japan by simultaneous inversion of 3-D velocities and geometry of the Conrad and Moho using comprehensive seismic data available from the present seismic networks (Fig. 6). The general feature in Moho depth variation is consistent with that by Zhao et al. (1990, 1992b), namely the NS trending belt of deep Moho in the central part of NE Japan and an area of the deepest Moho (>38–40 km) east of the ISTL in the central part of Honshu (see also Fig. 1). In Fig. 7, we notice a zone of shallow Moho (less than 30 km) in northern Kyushu, which represents crustal thinning associated with tensional stress field in this region (Katsumata, 2010). Such a tendency is consistent with the result from the active-source seismic experiment in eastern Kyushu (Profile F, Ohtsu, 2011). Furthermore, Katsumata (2010) provided Moho structures in the Izu and Ryukyu Arcs. The Moho depth in northern Izu Arc is around 30–32 km, which is consistent with result of the marine profile (Profile I, Kodaira et al., 2007). In the northern most part of the Okinawa Trough, the Moho depth is obtained as 28–32 km, which also agrees with those from Profiles J1 (Iwasaki et al., 1990) and Profile K (Nakahigashi et al., 2004). Matsubara et al. (2008) presented 3-D velocity structure beneath the Japanese islands assuming finer grid spacing as compared with the previous studies (Zhao et al., 1992a,b). At depth levels of 30–40 km, low velocity anomaly is clearly imaged along the volcanic front. In NE Japan, it is evident that the pattern of this low velocity is well consistent with the deeper Moho area (>34 km) by Zhao et al. (1990, 1994), Nakajima et al. (2002) and Katsumata (2010).

The Moho depth variations were also investigated by several authors using the receiver function (RF) analysis method (e.g. Igarashi

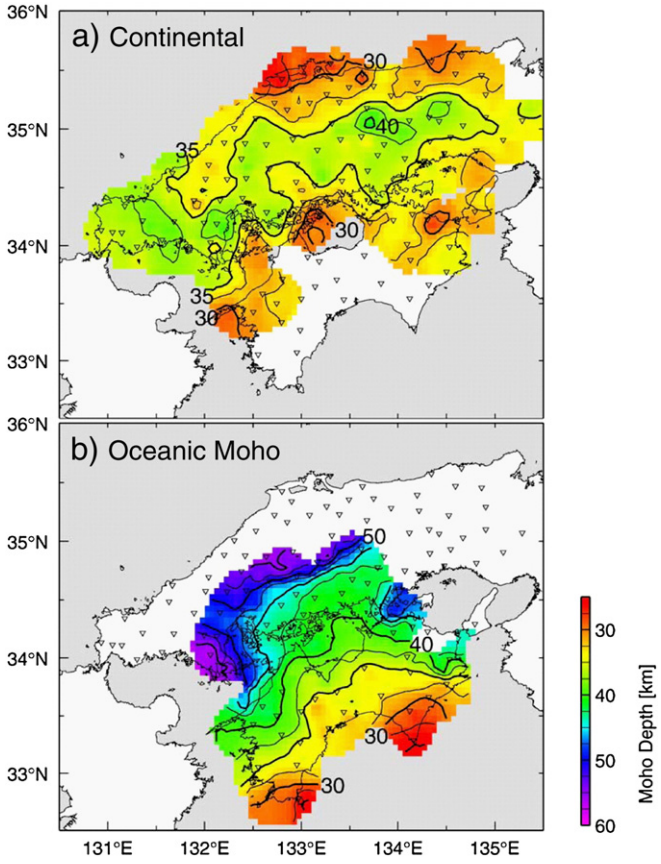

Fig. 8. Moho depth map in the SW Japan Arc after Shiomi et al. (2006). Inverted triangles denote seismic stations used in the analysis. (a) Island arc Moho. (b) Oceanic Moho.

et al., 2011; Shiomi et al., 2004, 2006; Yamaguchi et al., 2003). Igarashi et al. (2011) presented a depth distribution of the top of the upper-mantle (Fig. 7). In the NE Japan, the main features of their findings are consistent with those from tomographic studies (Matsubara et al., 2008; Zhao et al., 1992a). In general, their Moho depths tend to be larger than those from the tomography analysis or the active-source seismic experiments. For example, the Moho profile for A–A′ in Fig. 7 is plotted in the structural section from Profile C2 (Fig. 4b). Plausible explanation for this difference is Vp/Vs variation within the crust (Igarashi et al., 2011). Alternative explanation is that the Moho forms a transition zone with a depth-variable gradient, rather than a single velocity discontinuity (see Section 6.1). In the active-source seismic survey along Profile C2 (Iidaka et al., 2004), no clear PmP phase was observed, and the Moho depth was constrained from Pn phases. This result likely represents the upper part of the Moho transition zone with a more gradual velocity change with depth. The RF analysis, on the other hand, is very sensitive to the velocity contrast, and the deeper Moho from the RF analysis by Igarashi et al. (2011) may reflect the presence of a deeper strong velocity contrast within this transition zone. Alternatively, some places with the deeper Moho along the coastlines of Pacific/Philippine Sea Plates may represent the Moho of the subducted oceanic plate.

For the SW Japan Arc, Shiomi et al. (2006) presented the island arc Moho and oceanic Moho (Fig. 8). In Fig. 4a, their Moho depth is superimposed on the structural section along Profile E2. The oceanic Moho determined from the receiver function analysis agrees well with that from the active-source seismic experiment. On the other hand, there exists significant discrepancy in the island arc Moho. Actually, the Moho from receiver function analysis is very deep (more than 40 km) beneath the Inner zone (the Chugoku District), which is in a marked contrast to those of the active source experiment by Kurashimo et al. (2002, 2004), Ito et al. (2009) and tomography analysis by Katsumata (2010). The receiver function analysis by Igarashi et al. (2011) also shows the thickening of the crust beneath the

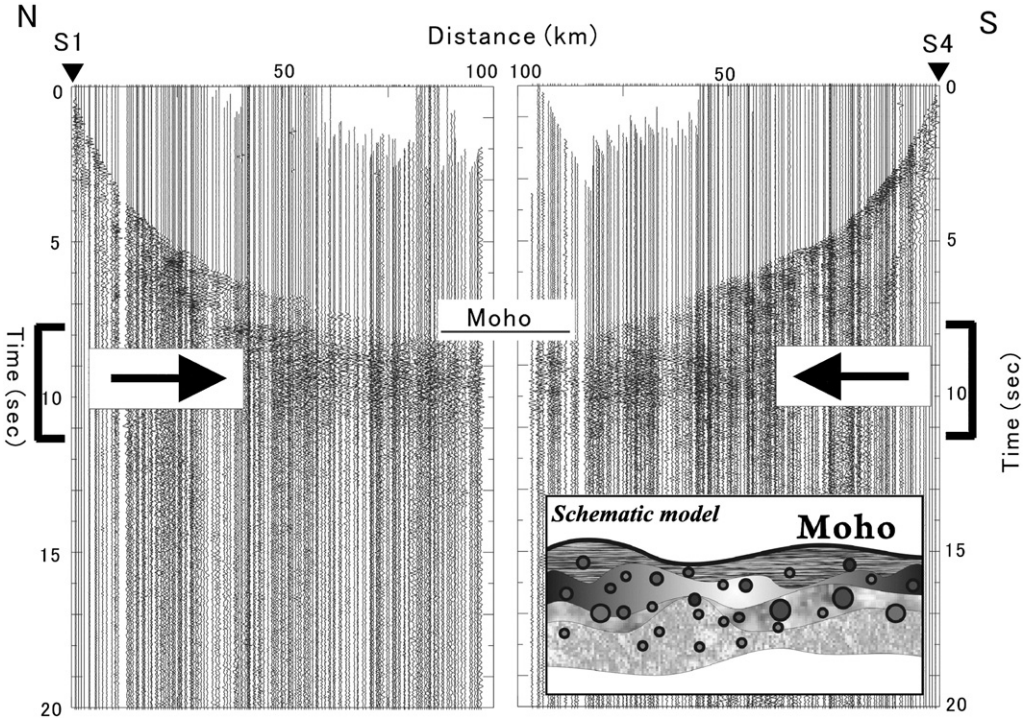

Fig. 9. NMO section for Profile B in Fig. 1, after Iidaka et al. (2006). Records from northernmost and southernmost shots are used. As indicated by arrows and square brackets, it is very clear that PmP wave has a long coda, which indicates complicated reflecting structure below the Moho. Schematic model explaining the long-duration PmP coda is also shown, characterized by a number of scatterers distributed beneath the Moho.

Chugoku District. The reason for this discrepancy has not been clarified as yet. One possibility is the transition zone structure around the Moho affected by the volcanic activity as mentioned above (see also Section 3.5.1).

3.5. Regional structural features of Moho boundary

3.5.1. Heterogeneity around Moho beneath arc crust

As described in the previous sections, the Pn velocity under the Japanese islands is estimated to be low (7.5–7.9 km/s). Fig. 9 shows a NMO section from Profile B, in a stable forearc block of the NE Japan Arc. In this record, PmP phase is characterized as a wave train with a duration time of 2–3 s. Such a reverberation was also found in the SW Japan Arc (Hashizume et al., 1981; Iwasaki et al., 2002; RGES, 1995; Takeda, 1997). From seismic array data collected on Profile e, Hashizume et al. (1981) interpreted such a wave train to be generated by multi-path reflection from irregular Moho geometry with characteristic dimension of several kilometers. Iwasaki et al. (2002) and Iwasaki and Sato (2009) pointed out the possibility for the existence of transition zone from lower crust to Moho, probably formed in the deformation/evolution process of the original crust through the back-arc spreading or the present-day volcanism.

Iidaka et al. (2006) investigated the structural inhomogeneity for explaining such "non-transparent Moho" observed for Profile B (Fig. 1) in NE Japan (Iwasaki et al., 1994; RGES, 1992). According to their results, the distorted Moho boundary structure as proposed by Hashizume et al. (1981) or the horizontal layering beneath the Moho does not explain the observed waveforms. A preferred model is that the seismic scatterers are distributed in the uppermost mantle as shown also in Fig. 9. According to the tomographic results by Zhao et al. (1992b) and Nakajima et al. (2001), magma is produced at depths of about 150 km just above the subducting slab and rises to the shallower levels (e.g. Nakajima et al., 2001, 2005). The magma, which has risen to the mantle wedge, stays just below the Moho boundary because of density balance. As components of magma segregate, light components of the magma rise again inside the crust, while the remaining components remain at the uppermost mantle level. The remaining part of the segregated magma is a candidate for the scatterers observed by seismological studies. The scatterers located in the uppermost mantle might be the remnants of magma segregation in the uppermost mantle.

3.5.2. Fluid transport and structure of the mantle wedge

In the SW Japan Arc, Matsubara et al. (2009) identified good correlation between locations of non-volcanic tremors and high Vp/Vs zone around the mantle wedge. Such a relationship is dominated by the dehydration and serpentinization processes in the subducted lithosphere and the mantle wedge (e.g. Kamiya and Kobayashi, 2000). This structural feature was more clearly revealed from combined analysis of active and passive source data in the eastern part of the SW Japan (Tokai region, see Fig. 1). In this area, M8 class megathrust event is expected to occur (Ando, 1975; Mogi, 1981, see region S1 in Fig. 1). Furthermore, the prominent crustal movement observed northwest of the expected fault area from 2000 to 2005, is considered to be the evidence for a long-term slow slip occurring on the plate boundary (Ozawa et al., 2002, a region S2 in Fig. 1). Combining the active source data and natural earthquake data (Profiles C1–3), Kodaira et al. (2004) and Kato et al. (2010) delineated a very low Vp/Vs part within the subducted oceanic crust just beneath the slow slip region (Fig. 10). This portion is considered to be a subducted ridge, in which fluids are trapped by the dehydration process. The fluids are believed to be overpressured by impermeable high velocity cap rock situated just above the plate boundary. Such overpressurization is responsible for a change in frictional property of the plate boundary to the conditionally stable state, which yields a wider slow slip area. The Vp/Vs value downward of the ridge is still high but the strength of its anomaly is diminished. It is also noted that the tip of the mantle

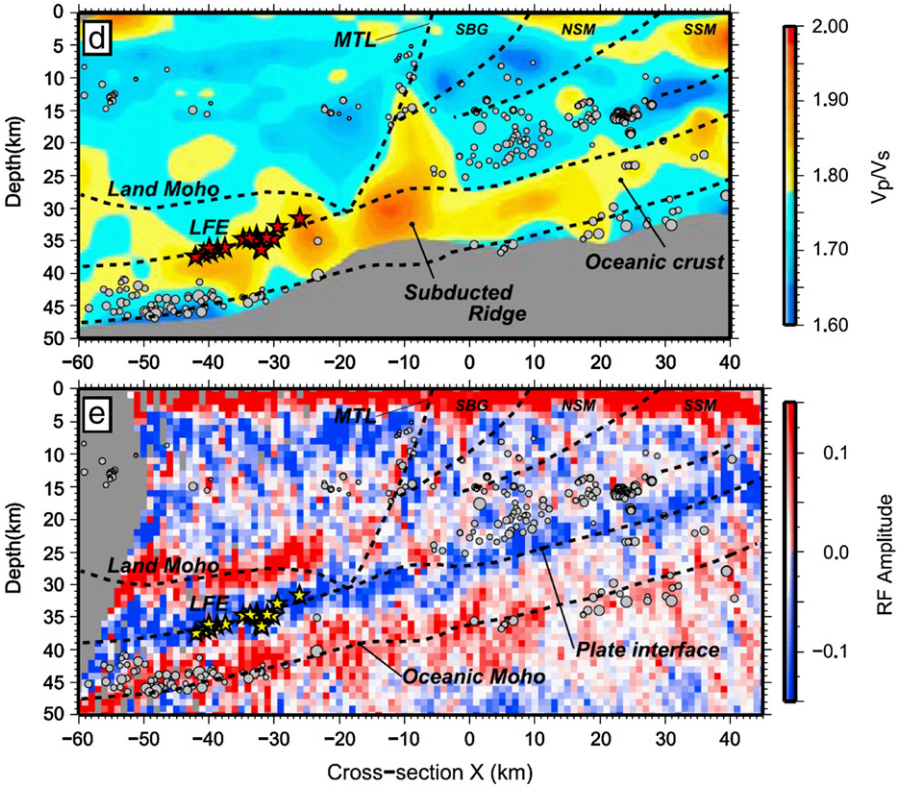

Fig. 10. Crust and upper-mantle section in the Tokai Dist. From passive seismic source (Profile C3 in Fig. 1) after Kato et al. (2010) by permission of American Geophysical Union. The upper plate shows Vp/Vs structure derived from tomography analysis. The lower plate is receiver function image. Major structural boundaries are indicated by dashed lines. LFE: low frequency earthquake.

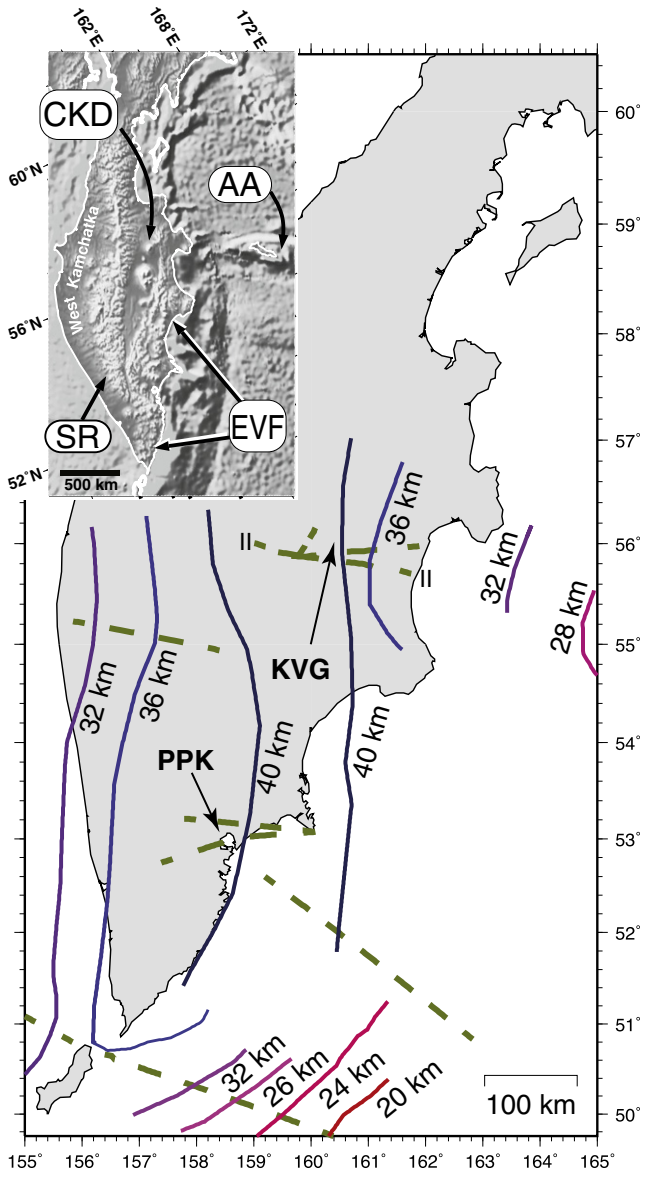

Fig. 11. Location of DSS profiles (dashed lines) and crustal thickness contours (solid lines) interpreted by Bulin (1977). Marked on the figure are locations of the city of Petropavlovsk-Kamchatsky (PPK) and the Klyuchevskoy Volcanic Group (KVG). The inset shows tectonic units discussed in Section 4.1: AA — Aleutian Arc, EVF — Eastern Volcanic Front, CKD — Central Kamchatka Depression, and SR — Sredinnyi Range.

wedge shows a relatively high Vp/Vs value. So, in this part, the fluids still remain within the oceanic crust but their partial leakage into the mantle wedge occurs, inducing serpentinization there. This is a reason for a decrease in seismic velocity and an increase in Vp/Vs value in the toe of the mantle wedge. Low frequency earthquakes (LFEs) are occurring beneath this serpentinized mantle wedge. So, the transport mechanism of fluids dehydrated from the subducted slab to the overriding arc crust/mantle controls the physical property of plate boundary, providing a key to understanding a wide range of slip phenomena, from slow-slip to megathrust.

4. Moho studies and constraints in Kamchatka

4.1. Brief overview of Kamchatka tectonic setting

The Kamchatka peninsula has recently been a subject of a special volume (#172) in the AGU Geophysical Monograph series (Eichelberger et al., 2007), and has also figured prominently in the AGU Geodynamics Series volume # 30 (Stein and Freymueller, 2002). Our brief summary of Kamchatka tectonics is derived largely from contributions within these two collections, with a few more recent additions to the plate tectonic reconstructions. It is composed with an aim of placing observations of crustal thickness and the nature of the crust–mantle boundary in the context of likely geodynamic processes.

A key element of the Kamchatka peninsula tectonic structure today is the existence of three distinct volcanic fronts (Fig. 11 inset). The western volcanic front (WVF), often referred to as "Central", a translation of its Russian name, "Sredynniy" (SR in Fig. 11), is nearly extinct. Volcanic formations associated with it extend along most of the peninsula. The presently active eastern volcanic front (EVF) stretches along the eastern coast, from the southern tip of Kamchatka to the junction with the Aleutian Arc at ~56°N. Between these two regions of elevated topography lies a sediment-filled Central Kamchatka Depression (CKD), which hosts a cluster of extremely active volcanoes in its northern part (55°–57°N). In geodynamic terms, the EVF, together with the Kurile Arc to the south, is directly linked to the subduction of the Pacific plate. It is a "textbook" subduction zone, with relatively rapid (over 8 cm/yr) near-normal convergence, steep (over 50°) angle of subduction, and the lithospheric slab extending all the way to the transition zone (cf. Syracuse and Abers, 2006). In its northernmost part, at the junction with the Aleutian Arc, the shape of the subducting Pacific plate changes, with much shallower angle of descent (~35°, Gorbatov et al., 1997) and only a limited (<200 km) reach into the upper mantle. An association of this bend in the Pacific slab beneath Kamchatka and the location of the CKD volcanoes above it has been a subject of numerous, and divergent, attempts at geodynamic interpretation (e.g., Avdeiko et al., 2007; Levin et al., 2002b; Nikulin et al., 2012; Portnyagin et al., 2005). The largely extinct WVF is clearly associated with westward subduction of the oceanic plate. Avdeiko et al. (2007) summarize arguments in favor of this plate being the Pacific plate, while Park et al. (2002) propose a reconstruction where the WVF is formed by subduction of young oceanic lithosphere from beneath the Komandorsky Basin (presently the westernmost part of the Bering Sea). These different scenarios rely on interruption of subduction (Avdeiko et al., 2007) or the migration of a triple junction between Pacific, North America (or Okhotsk) and Eurasia plates (Park et al., 2002).

On the basis of their formation age, three major elements are recognized within the Kamchatka peninsula, the western "backbone" predating volcanic activity, and two accreted volcanic terranes. The backbone, comprising the western coast and the foundations of the WVF, is thought to be of continental origin, with Siberian affinity (in the sense that rocks derived from areas further west are found within the metamorphosed sediments forming the backbone, Bindeman et al., 2002). The Olyutorsky (Bogdanov et al., 1990; Hourigan et al., 2009) or Achaivayam–Valaginian (Konstantinovskaya, 2001; Shapiro, 1995) terrane collided with the backbone at ~45 Ma, and presently covers most of the peninsula. The Kronotsky terrane (Konstantinovskaya, 2001) forms the prominent east-facing peninsulas of Kamchatka, and has arrived within the last 10 Ma. The mode of arrival of this easternmost terrane factors into the discussions of the EVF origin mentioned above. A time-lapsed accretion with southern peninsula accreting almost 10 Ma earlier than the northern one (Park et al., 2002; also Lander and Shapiro, 2007) will favor a triple-junction migration model. One unresolved issue in Kamchatka is whether any part of its lithosphere is older than ~50 Ma. Arguments for older origin of some part of western Kamchatka are presented by Bindeman et al. (2002), while a view that western Kamchatka crust consolidated synchronously with the Olyutorsky arc accretion has been elaborated most recently by Hourigan et al. (2009).

Relevant to the subject of the present review are two broad inferences about the tectonic history and present-day conditions in Kamchatka.

Firstly, most of the Kamchatka landmass is composed of terranes with island-arc origin that have formed elsewhere prior to their

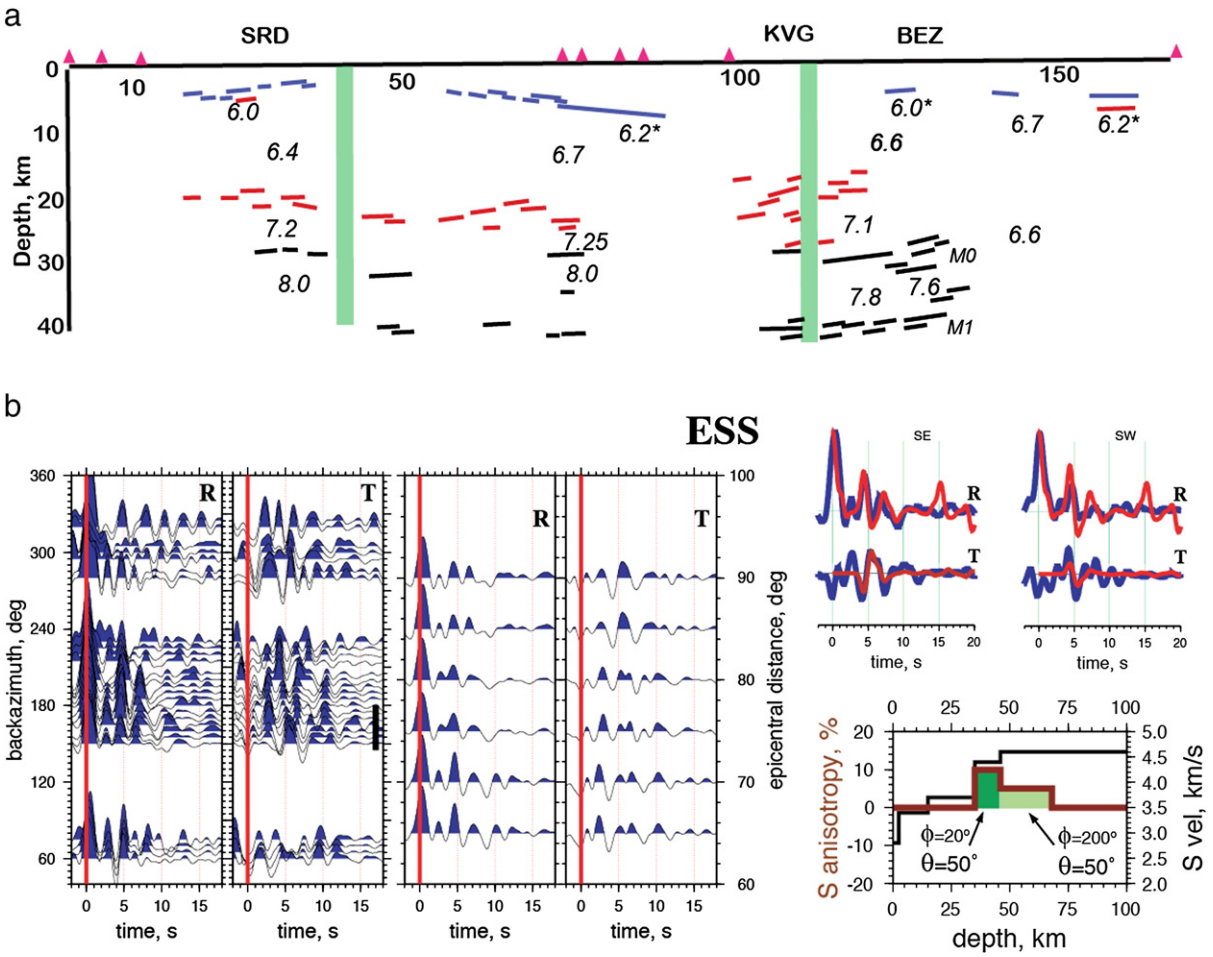

Fig. 12. Data examples: a) a line drawing of the DSS profile II across central Kamchatka (location shown in Fig. 11), adapted from Utnasin et al. (1975). The same profile is shown in Fig. 1a of Balesta et al. (1977). Distances along the profile and depth values are in km; triangles on top of the profile mark shot points; line segments represent refracting or reflecting boundaries color coded by their interpretation: blue — top of the consolidated basement, black — crust–mantle transition, red — other boundaries (shallow boundaries present in the original publication are omitted here); vertical green bands show interpreted "deep fault zones"; values of P wave speed, in km/s, represent interval velocities except for values with an asterisk which represent refracted wave velocity. Marked on the profile are projected locations of the Sredinny Range (SR), Klyuchevskoy volcanic group (KVG), and the Bezymyanny volcano (BEZ). b) Receiver function analysis and modeling results for site ESS (Fig. 12, inset) in central Kamchatka, adapted from Levin et al. (2002a). Earthquakes observed over a year-long period in 1998–1999 are used to construct a composite wavefield. Two frames on the left show backazimuthal gathers of receiver functions (RFs), for radial and transverse components, respectively. A thick solid line in the transverse RF frame denotes the backazimuthal range used for the epicentral sweep. Two frames on the right denote the epicentral gathers of RFs, for radial and transverse components, respectively. Radial pulse at 5 s is clear in all epicentral distance ranges, and moves out to shorter times for steeper incident rays (larger distances). Results of forward modeling for station ESS are shown in the right part of the plot. In waveform plots blue lines show data and red lines show reflectivity synthetics computed using the methodology described in Levin and Park (1997). On the lower diagram the change of V_S with depth is shown by a black line, while variations in peak-to-peak V_S anisotropy are shown by the red line. Two anisotropic layers in the model are shaded and orientations of the respective symmetry axes (phi — tilt from vertical, theta — azimuth from North) are marked on the plot.

accretion to Kamchatka over the last 50 Ma. With a possible exception of a region in south-central Kamchatka that may be Mesozoic or even older, the crust of Kamchatka is relatively young and has not been a part of a stable continent.

Secondly, most of Kamchatka has been affected by subduction processes for the last 50 Ma, thus the upper part of the mantle beneath it has likely been significantly altered.

4.2. Constraints on the Moho depth and properties

4.2.1. Active-source methods

In Kamchatka, DSS surveys were performed in two broad transects, centered on major volcanic groups and settlement centers. One transect crossed southern Kamchatka at the latitude of the Avachinsky volcano group and the main city of Petropavlovsk-Kamchatksy, while another was performed at the latitude of Klyuchevskoy volcano and the settlement of Klyuchi. Fig. 11 shows locations of the profiles, as summarized by Bulin (1977). Other publications presenting diagrams of observational geometry are Utnasin et al. (1975), Anosov et al. (1976), Balesta et al. (1977) and Balesta and Gontovaya (1985). It is worth noting that presentation of primary data was not an accepted practice in the Soviet Union of 1970s and 1980s, with only schematic drawings presented in available publications.

The logic of reporting an individual value of the Moho depth on the basis of a DSS profile is as follows. Results of interpreting a DSS profile are presented in a form of a distance–depth plot along the profile, with positions of reflecting surfaces and values of speed in layers between them marked (see Fig. 12). Position of the Moho is chosen to lie between layers with speeds less than 7.0 km/s and more than 7.8 km/s, respectively (Balesta et al., 1977). Bulin (1977) summarized Moho depth estimates from all DSS profiles available for Kamchatka. These estimates are shown in Fig. 13. Offshore Kamchatka values are generally below 30 km, although two readings of 39 and 40 km are shown along a line extending eastward from Petropavlosk-Kamchatsky. A profile extending from the west coast inland shows a gradual deepening of the Moho from 32 to 39 km. Values between 38 and 40 km are also reported along the east coast of Kamchatka, beneath the volcanic front. In the vicinity of the Klyuchevskoy volcanic

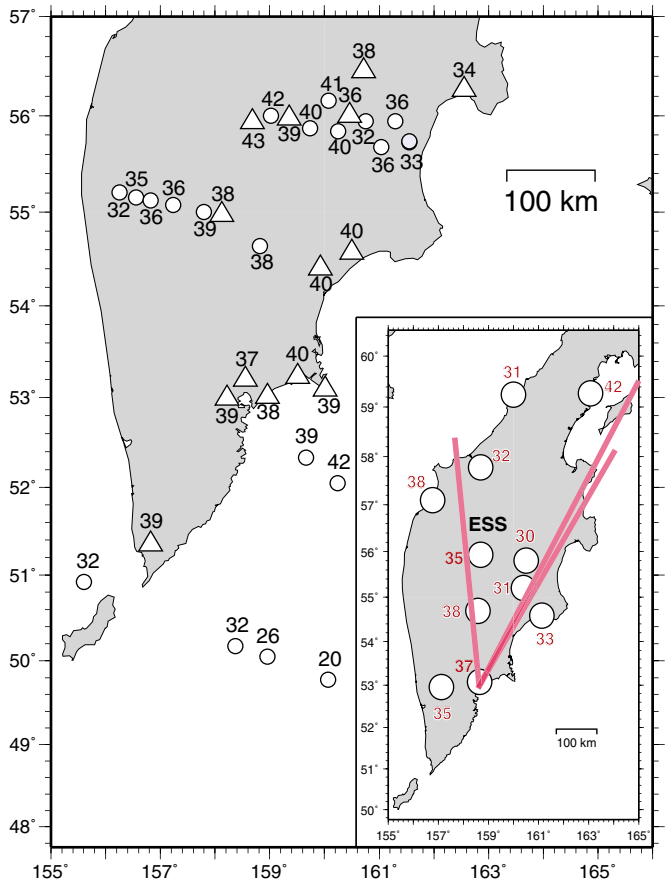

Fig. 13. Crustal thickness values for Kamchatka peninsula interpreted from DSS profiles and teleseismic P-to-S converted waves. Locations of crustal thickness estimates on the main map are as presented in Bulin (1977). Values shown by circles are based on a series of DSS profiles described in Utnasin et al. (1975), Anosov et al. (1976) and Balesta et al. (1977, 1985). Locations of profiles are presented in Fig. 11. Values shown by triangles are seismic observatories where timing of visually picked converted body waves from distant earthquakes was used to estimate crustal thickness. An inset shows crustal thickness values from more recent receiver function studies (Levin et al., 2002a; Nikulin et al., 2010) and ray paths from regional earthquakes (red lines) used in studies of surface wave dispersion by Shapiro et al. (2000) and Gordeev et al. (2009). The location of seismic station Esso (ESS) where analysis illustrated in Fig. 12b was performed is marked.

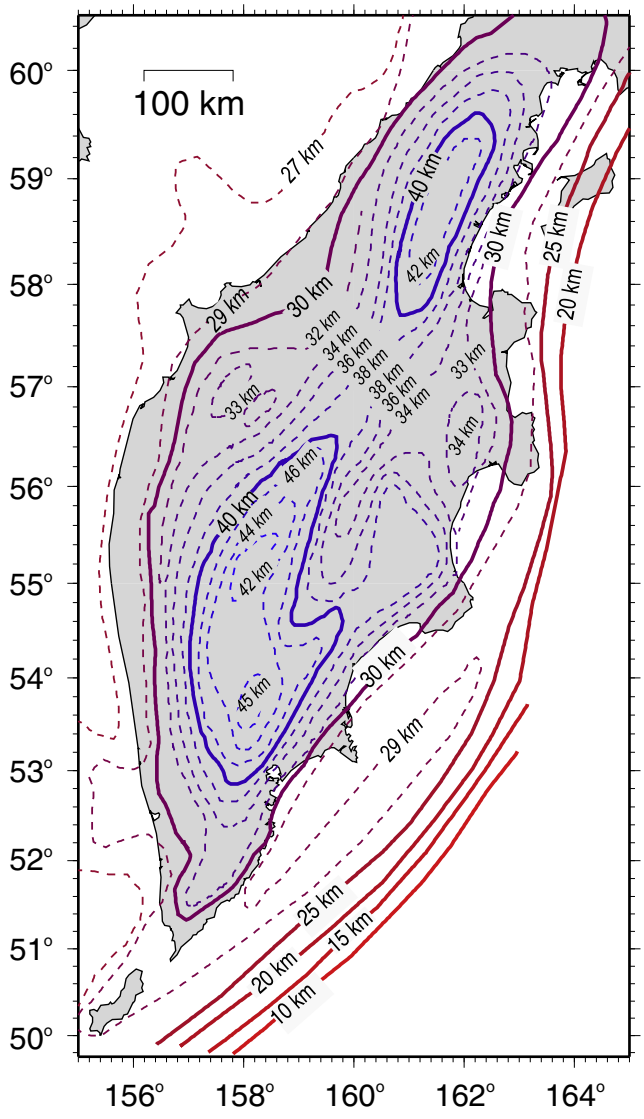

Fig. 14. Crustal thickness values derived from gravity studies of the Okhotsk sea basin, the Kuril Islands and the Kamchatka peninsula, originally presented in the publication of Baboshina et al. (1984)). Solid lines indicate contours in increments of 5 km. Dashed lines refer to smaller increment contour lines (marked).

group values appear inconsistent, with changes over 5 km in Moho depth between adjacent readings. We note that Utnasin et al., 1975 (see Fig. 12) and Balesta et al. (1977) show line drawings of the DSS line beneath this region, with multiple candidate reflectors labeled "Moho", at different depths. Values reported by Bulin (1977) must reflect individual choices, however they are not reflected in the original papers.

4.2.2. P-to-S converted waves

A method used by a number of researchers in Kamchatka (Bulin, 1977; Zlobin et al., 2005) relies on visual recognition of the P to S converted waves in clear records of teleseismic earthquakes. Once the phases are identified and picked, depth to the Moho is estimated on the basis of standard relationships that take into account speeds of P and S waves in the crust. In case of the study of Kamchatka reproduced in this report, a relationship derived elsewhere was used (Bulin, 1977). Levin et al. (2002a) and Nikulin et al. (2010) used modern receiver function methodology to estimate Moho depth beneath networks of temporary broadband seismic stations across the Kamchatka peninsula. In both studies the ratio of P to S wave speed was taken to be 1.75. Results obtained by Bulin (1977) are shown, along with the DSS results, in the main map of Fig. 13. Most values reported are in 35–40 km range, both in the central part of Kamchatka peninsula and along the eastern coast. Moho depth values based on receiver function methodology obtained by Levin et al. (2002a) and Nikulin et al. (2010) are shown in the inset. Values range from 30 to over 40 km.

4.2.3. Dispersion of surface waves from earthquakes at regional distances

We are aware of two studies of crustal thickness of Kamchatka using this approach, both by N. Shapiro and colleagues (Gordeev et al., 2009; Shapiro et al., 2000). In both cases earthquakes in the northern part of Kamchatka peninsula were recorded by the seismic station in the south (Petropavlovk-Kamchatsky, see schematic ray paths in the inset of Fig. 13). Crustal thickness estimates from these studies are 36 and 32 km, respectively.

4.2.4. Gravity

A detailed map of crustal thickness derived on the basis of gravity field observations is included as an inset in the tectonic map of the Sea of Okhotsk Region (Bogdanov and Khain, 2000). The map, redrawn in the common projection in Fig. 14, is attributed to the group of authors lead by V. A. Baboshina. The original work was presented in Baboshina et al. (1984), in an internal report of GAZPROM when it was an oil and

gas industry research institute. The specific formulae used to convert gravity field strength to crustal thickness are not presented. Most notable feature of this map is a region of thick (40 + km) crust in central and northern Kamchatka, largely coincident with the axis of the peninsula. This elongated region of thick crust is interrupted by a zone of apparent thinning extending SE–NW across the peninsula at the 56–57° latitudes, approximately along the projection of the Aleutian arc. Crustal thickness decreases towards the coasts of the peninsula, reaching values of 25–30 km at the shoreline.

4.3. Upper mantle properties beneath Kamchatka

Constraints on the properties of the uppermost mantle beneath Kamchatka are available from observations of regionally propagating body and surface waves, from imaging studies, and from receiver function studies. All are limited in their spatial resolution by the small number of observing locations, largely restricted to the population centers and the areas south of the junction with the Aleutian Arc. A key finding in the majority of studies is that the seismic velocities beneath Kamchatka are very low. This was a prominent early result obtained by Fedotov and Slavina (1968) on the basis of regional earthquakes studies in the EVF, who reported speeds as low as 7.6 km/s, more commonly 7.8 km/s, along paths parallel to the eastern coast of Kamchatka. A tomographic study of the uppermost mantle by Gorbatov et al. (1999) yielded average P wave speed values between 7.37 and 7.64 km/s in the depth range 35–75 km. Lateral variations in wave speed constrained by that study showed clear association of low wave speed with the EVF. Similar results are obtained by Gontovaya et al. (2008) with a much larger data set. Regional surface wave dispersion studies by Shapiro et al. (2000) and Gordeev et al. (2009) yield estimates of shear wave speed of 4.2 and 4.1 km/s, respectively. Similarly low wave speed is apparent in results of the surface wave tomography (e.g., Levin et al., 2002b). Finally, the P-to-S converted wave study of a few locations by Levin et al. (2002a)) showed clear evidence of anisotropy (and by inference — systematic rock texture) associated with the crust–mantle transition (see Fig. 12). The orientation of symmetry axes was close to trench-normal along the eastern coast of Kamchatka, while sites inland and on the west coast did not seem to be systematic.

4.4. Comparison of results from different techniques

There are important similarities and discrepancies that should be noted in different datasets. These differences are expected to a degree given that the DSS studies reflect P-wave structure of the crust, while surface wave dispersion and P-to-S converted wave observations are sensitive to the S wave speed. Furthermore, the frequency content of the observations is also significantly different between various techniques. DSS studies and work on converted waves utilized short period sensors, and thus data from these studies are sensitive to smaller scale features. On the other hand, broadband receiver function analysis, and especially surface wave dispersion studies reflect more gradual changes in properties.

The overall estimate of crustal thickness under Kamchatka as being between 30 and 40 km is consistent in all published studies. Presence of thicker crust along the axis of the peninsula, and a decrease of the Moho depth towards the western shore appear in DSS, receiver function and gravity studies.

Presence of the somewhat thinner crust (~30–35 km) at the latitude of Klyuchevskoy volcanic group is evident in the gravity-derived map (Fig. 14) and also in the receiver function studies of Levin et al. (2002a) and Nikulin et al. (2010) while DSS results and Bulin (1977) interpretation of the visually identified P-to-S converted waves show larger values. Gravity results suggest thicker crust in northern part of Kamchatka, which is also implied by one site on the western coast analyzed by Levin et al. (2002b). We note that the seismic result was viewed as questionable by the authors.

A significant discrepancy in Moho depth estimates is seen along the eastern coast of Kamchatka and beneath the Klyuchevskoy volcanic group. This discrepancy is not surprising given that the presence of at least two candidate "Moho" boundaries has been reported by DSS studies (Utnasin et al., 1975; Balesta et al., 1977; see Fig. 12), and has also been noted in receiver function analysis of Nikulin et al. (2010)).

It is interesting to speculate on the causes of the differences in Moho depth estimates between surface waves, receiver functions and earlier high-frequency studies summarized by Bulin (1977). A scenario that would explain thinner crust seen by longer-wavelength measures would involve a gradual transition from crustal to upper-mantle rocks starting at ~30 km depth and occurring over ~10 km, with additional sharper (few km in thickness) features closer to 40 km depth. A notion of gradual Moho boundary beneath Kamchatka is long-standing, and may be traced to initial DSS studies publications (e.g., Balesta et al., 1977).

5. Discussion and conclusions

This review presented the Moho and uppermost mantle structures beneath the Kamchatka peninsula and Japan which have been developed as island arcs along the eastern margin of the Asian continent. Here, we also included the results in the Izu–Bonin Arc. Key observations are summarized in Table 1. The Moho and the upper mantle structures in the NE Japan and SE Japan Arcs have been investigated well both from active and passive seismic source studies including marine expeditions. The Moho depth in the NE Japan is ranging from 30 to 40 km (Igarashi et al., 2011; Katsumata, 2010; Zhao et al., 1990, 1992b). Almost parallel to the present volcanic front, there exists a belt of deep Moho (34–36 km) with a lower Pn velocity (7.5–7.7 km/s) (Iwasaki et al., 2001; Zhao et al., 1990, 1992b). Amplitude analysis of the PmP phase indicates that the Moho beneath the NE Japan Arc is not a simple velocity contrast, but rather a gradual transition. This structural transition is well modeled by scatterers distributed in the uppermost mantle (Iidaka et al., 2006), which may express structural heterogeneity derived in the formation process of crustal materials from magma rising in the mantle wedge. Toward the backarc side, remarkable crustal thinning is recognized. Actually, the Moho depth decreases from 35 km beneath the central part of NE Japan to 18 km beneath the Sea of Japan (Iwasaki et al., 2001). This thinning is evident in the upper crust, while the lower crust remains constant in thickness. This may be explained by the continuous magmatic underplating beneath the rifted crust. An alternative explanation is that the back-arc spreading progressed in a simple shear mode, allowing the lower crustal thickness to remain unchanged.

The Moho in the SW Japan Arc is also at a depth of 30–40 km (Igarashi et al., 2011; Ito et al., 2009; Katsumata, 2010; Kurashimo et al., 2002, 2004; Shiomi et al., 2004; Zhao et al., 1992b). The Pn velocity is 7.7–7.8 km/s, slightly higher than that in the NE Japan. This value was mostly sampled in the eastern half of the SW Japan Arc, where the recent volcanic activity has been less effective. Fluids expelled from the subducted oceanic lithosphere (the PHS plate) play an important role in controlling the structure of the mantle wedge as well as frictional properties on the subducted plate boundary. As these fluids leak into the mantle wedge they induce serpentinization there, transforming original mantle materials to those of lower velocity and higher Vp/Vs. The crustal thinning of the SW Japan Arc is similar to the case of the NE Japan Arc. Namely, notable decrease in upper crustal thickness is recognized in contrast with the lower crust with more or less constant thickness. Such a deformation style is also seen in the Okinawa Trough behind the Rukyu trench–arc system, and may be a common for the backarc spreading occurring in the middle part of the Asian continental margin.

Table 1
Summary table for the review paper describing Kamchatka and Japan Moho studies.

	Kamchatka	Northeastern Japan	Central Japan	Southwestern Japan	Izu–Bonin
Forearc					
Moho depth	10–32 km	20–30 km	25–30 km	~30 km	18 km
Moho nature	Eastward decrease in Moho depth	Eastward decrease in Moho depth	–	–	–
Crustal P wave speed	6.2–6.7 km/s	5.0–7.0 km/s	5.7–6.7 km/s	5.7–6.6 km/s	5.9–7.4 km/s
Crustal S wave speed	3.3–3.9 km/s	–	3.3–4.0 km/s	3.3–4.0 km/s	–
Upper mantle P wave speed	–	7.9–8.1 km/s	7.8–7.9 km/s	7.8 km/s	7.7 km/s
Volcanic arc					
Moho depth	30–40 km	30–40 km	30–40 km	30–40 km	10–32 km
Moho nature	A gradual transition from the crust to the mantle	(1) NS trending belt of deep Moho and low Pn along the QVF; (2) a gradual transition from the crust to the mantle	A gradual transition from the crust to the mantle	A gradual transition from the crust to the mantle	A gradual transition from the crust to the mantle
Crustal P wave speed	6.6–7.1 km/s	5.7–7.0 km/s	5.5–6.8 km/s	5.7–6.6 km/s	6.0–7.6 km/s
Crustal S wave speed	3.5–3.8 km/s	3.3–4.1 km/s	3.3–4.1 km/s	3.3–4.1 km/s	–
Upper mantle P wave speed	7.4–7.8 km/s	7.5–7.7 km/s	7.6–7.9 km/s	7.6–7.8 km/s	7.8–8.0 km/s
Backarc					
Moho depth	27–45 km	18–30 km	–	15–20 km	10–15 km
Moho nature	(1) Westward decrease in Moho depth; (2) sharp Moho along western coast	(1) Westward decrease in Moho depth; (2) 20–30 km wide lateral transition in Pn velocity	–	northward decrease in Moho depth	westward decrease in Moho depth
Crustal P wave speed	6.0–7.2 km/s	5.6–6.8 km/s	–	5.6–6.9 km/s	5.6–7.5 km/s
Crustal S wave speed	3.5–3.8 km/s	–	–	–	–
Upper mantle P wave speed	8.0 km/s	8.0 km/s	–	8.0 km/s	7.9–8.1 km/s

The Moho and uppermost mantle structures beneath the southern part of the Kamchatka have a lot of similarities to those beneath the NE Japan Arc. Earlier DSS investigations (Anosov et al., 1976; Balesta and Gontovaya, 1985; Balesta et al., 1977; Bulin, 1977; Utnasin et al., 1975) and converted wave analyses (Bulin, 1977; Zlobin et al., 2005) show that Moho is situated at a depth of 38–40 km along the east coast of Kamchatka, that is beneath the volcanic front, but decreases to about 32 km near the west coast.

Moho depth values based on modern receiver function methodology obtained by Levin et al. (2002a) and Nikulin et al. (2010) are also ranging from 31 to over 38 km. Frequency content and directional stability of pulses suggest that Moho is a fairly simple boundary under the western coast of Kamchatka, while in the Central Kamchatka Depression and especially along the eastern coast it is likely gradational. Intense crustal multiples make receiver function analysis very difficult at all sites along the eastern coast, thus crustal values here are least reliable. Uppermost mantle material beneath the Moho is complex, with additional impedance contrasts that are likely anisotropic in their properties being present under the entire Kamchatka peninsula. The dominant anisotropy-inducing fabric varies from site to site along the west coast, but is almost universally trench-normal along the east coast.

The seismic velocities beneath Kamchatka are very low (7.4–7.8 km/s for P-wave and 4.1–4.2 km/s for S wave) (Fedotov and Slavina, 1968; Gontovaya et al., 2008; Gorbatov et al., 1999; Gordeev et al., 2009; Levin et al., 2002b; Shapiro et al., 2000). Also, gradual structural change is recognized around the Moho beneath the active volcanoes. These features are quite similar to those in NE Japan Arc. According to tomographic image beneath the NE Japan (e.g. Nakajima et al., 2001, 2005; Zhao et al., 1992b), a large scale low velocity anomaly is found just above the subducted Pacific Plate, whose uppermost part forms a low Pn velocity belt beneath central NE Japan. This anomaly, characterized by 5–10% velocity reduction and high Vp/Vs ratio, descends westward to a depth of 150 km, almost parallel to the Pacific Plate. This image probably represents a part of the upwelling magmatic flow associated with the secondary convection by the plate subduction (Hasegawa and Nakajima, 2004). Such a large-scale low velocity anomaly is also seen in the mantle wedge of Kamchatka, indicating the upwelling of magmatic flow mentioned above may be responsible for the common feature of the Moho and uppermost mangle structure beneath the NE Japan and Kamchatka (Nakajima et al., 2005).

The Izu–Bonin Arc has been formed in an intraoceanic convergent margin in contrast with the NE Japan and SW Japan Arcs built on the continental crust. Several structural sections crossing the arc show the remarkable variation in Moho depth from the trench to the backarc side. In the southern part of the Izu–Bonin Arc system (Takahashi et al., 2009), for example, the crustal thicknesses of the forearc (the Ogasawara (Bonin) ridge), current volcanic arc and backarc are 18, 25 and 16 km, respectively.

The Moho depth decreases on both sides of the arc where the effect of rifting is significant, and the crust is reduced in thickness by 50–60%. Unlike in the NE and SW Japan Arcs, the lower crust with P wave velocity of 6.6–7.5 km/s is responsible for this thinning. It is also noted that a layer of relatively low velocity (7.5–7.6 km/s) is situated just above the upper mantle of the current volcanic arc or back arc. This structure is interpreted to be the crust–mantle transition zone formed by the accumulation of dense materials derived from the crust in the course of the crustal growth (Takahashi et al., 2009).

In the Moho depths presented in this review, there are some discrepancies from different methodologies and datasets. Such differences are expected to some degree because the controlled source studies reflect P-wave structure, while surface wave dispersion and P-to-S converted wave observations are sensitive to the S wave speed. It is also noted that the frequency content of the observations is significantly different between various techniques.

The other important source for the discrepancies is the complexity of the Moho structure itself. It is plausible that the Moho forms a transition zone in which material properties change more or less gradually from the crust to the upper mantle. For example, the Pn wave measurement may reflect the seismic velocity change within this transition zone, and yield a smaller thickness of the crust. Receiver function analysis, on the other hand, may reflect the sharpest velocity contrast within the crust–mantle transition zone or even in the upper

mantle below. So, present discrepancies in Moho structure estimated by different methodologies may provide a new key in 5–10% velocity reduction and high Vp/Vs ratio, clarifying unknown heterogeneities existing between the crust and upper-mantle.

Acknowledgements

The authors would like to thank the editors of the special volume for their initiative, encouragement and patience while this review was being prepared. The authors express their sincere thanks to Junichi Nakajima for his numerous comments on tomography research in the NE Japan. They also thank Toshihiro Igarashi for providing a high resolution map of the Moho depth constrained by RF analysis, used in Fig. 7 of this paper. Suggestions by Alexei Gorbatov and careful reading of the text by an anonymous reviewer helped us improve the presentation. VL and AN were supported in part by the NSF grant EAR-1015422.

References

Ammon, C.J., 1991. The isolation of receiver effects from teleseismic P waveforms. Bulletin of the Seismological Society of America 81, 2504–2510.
Ando, M., 1975. Possibility of a major earthquake in the Tokai district, Japan and its preestimated seismotectonic effect. Tectonophysics 25, 69–85.
Anosov, G.I., Veselov, O.V., Pavlov, Y.A., Portnyagina, P.V., Soinov, V.V., Utnasin, V.K., Fedorchenko, V.I., 1976. Structure and composition of the crust in Central Kamchatka. Soviet Geology 7, 25–38 (in Russian).
Aoki, H., Muramatsu, I., 1974. Crustal structure in the profile across Kinki and Shikoku, Japan, as derived from the Miboro and the Toyama explosions. Zisin 27, 104–109 (in Japanese with English abstract).
Aoki, H., Tada, Y., Sasaki, Y., Ooida, T., Muramatsu, I., Shimamura, H., Furuya, I., 1972. Crustal structure in the profile across central Japan as derived from explosion seismic observations. Journal of Physical Earth 20, 197–223.
Asano, S., Okada, H., Yoshii, T., Yamamoto, K., Hasegawa, T., Ito, K., Suzuki, S., Ikami, A., Hamada, K., 1979. Crust and upper mantle structure beneath northeastern Honshu, Japan as derived from explosion seismic observations. Journal of Physical Earth 27, S1–S13 (Suppl.).
Asano, S., Yamada, T., Suyehiro, K., Yoshii, T., Misawa, Y., Iizuka, S., 1981. Crustal structure on a profile off the Pacific coast of northeastern Japan by the refraction method with ocean bottom seismometers. Journal of Physical Earth 29, 267–281.
Avdeiko, G.P., Savelyev, D.P., Palueva, A.A., Popruzhenko, S.V., 2007. Evolution of the Kurile–Kamchatkan volcanic arcs and dynamics of the Kamchatka–Aleutian Junction. Volcanism and subduction: the Kamchatka Region. Geophysical Monograph Series 172, 37–55.
Baboshina, V.A., Tereschenkov, A.A., Kharakhinov, V.V., 1984. Deep Structure of the Sea of Okhotsk According to Geophysical Data, Overview Information. Vsesouzniy Nauchno-Issledovatelskiy Institute (VNII) Gazprom 3:41 . (in Russian).
Balesta, S.T., Gontovaya, L.I., 1985. Crustal structures in the Kamchatkan segment of the Pacific transition zone. Journal of Geodesy 3, 245–257.
Balesta, S.T., Farberov, A.I., Smirnov, V.S., Tarakanovsky, A.A., Zubin, M.I., 1977. Deep crustal structure of the Kamchatkan volcanic regions. Bulletin of Volcanology 40, 260–266.
Bindeman, I.N., Vinogradov, V.I., Valley, J.W., Wooden, J.L., Natal'in, B.A., 2002. Archean protolith and accretion of crust in Kamchatka: SHRIMP dating of zircons from Sredinny and Ganal massifs. Journal of Geology 110, 271–289. http://dx.doi.org/10.1086/339532.
Bogdanov, N.A., Khain, V.E. (Eds.), 2000. Tectonic Map of the Sea of Okhotsk Region (scale 1:250,000), with Explanatory Notes (171 pages). Institute of the Lithosphere of Marginal Seas, Russian Academy of Sciences, Moscow, Russia.
Bogdanov, N.A., Til'man, S.M., Chekhovich, V.D., 1990. Geology of the western Bering Sea region; chapter 3, Late Cretaceous–Cenozoic history of the Koryak–Kamchatka region and the Commander Basin of the Bering Sea [modified]. International Geology Review 32, 1185–1201.
Bulin, N.K., 1977. Deep structure of Kamchatka and Kuril Islands from seismic data. Soviet Geology 5, 140–148 (in Russian).
Eichelberger, J., Gordeev, E., Izbekov, P., Kasahara, M., Lees, J. (Eds.), 2007. Volcanism and Subduction: The Kamchatka Region. Geophysical Monograph Series, vol. 172. AGU, Washington, D.C. http://dx.doi.org/10.1029/GM172 (369 pp.).
Fedotov, S.A., Slavina, L.B., 1968. Estimation of longitudinal wave velocities in the upper mantle beneath north-western part of the Pacific and Kamchatka. Izvestiya Akademii Nauk Sssr Fizika Zemli 2, 8–31 (in Russian).
Gontovaya, L.I., Popruzhenko, S.V., Nizkous, I.V., Aprelkov, S.E., 2008. Upper mantle beneath Kamchatka and its relation to tectonics. Russian Journal of Pacific Geology 2, 165–174. http://dx.doi.org/10.1134/S1819714008020073.
Gorbatov, A., Kostoglodov, V., Sua'rez, G., Gordeev, E., 1997. Seismicity and structure of the Kamchatka subduction zone. Journal of Geophysical Research 102, 17883–17898.
Gorbatov, A., Dominguez, J., Suarez, G., Kostoglodov, V., Zhao, D., Gordeev, E., 1999. Tomographic imaging of the P-wave velocity structure beneath the Kamchatka peninsula. Geophysical Journal International 137, 269–279.
Gordeev, E.I., Droznina, S.Y., Shapiro, N.M., 2009. Structure of the crust and upper mantle within the area of triple junction between the Pacific, North American and Eurasian lithospheric plates. Proceedings of the Russian Academy of Sciences 428 (3), 392–396.
Gurrola, H., Baker, F.G., Minster, J.B., 1995. Simultaneous time-domain deconvolution with application to the computation of receiver functions. Geophysical Journal International 120, 537–543.
Hasegawa, A., Nakajima, J., 2004. Geophysical constraints on slab subduction and arc magmatism. The State of the Planet: Frontiers and Challenges in Geophysics. Geophys., Monogr. Ser., vol. 150. AGU, Washington, DC, pp. 81–94.
Hasegawa, A., Unimo, N., Takagi, A., 1978. Double-planed structure of the deep seismic zone in the Northern Japan Arc. Tectonopysics 47, 43–58.
Hashizume, M., Ito, K., Yoshii, T., 1981. Crustal structure of south-western Honshu, Japan and their nature of the Mohorovicic discontinuity. Geophysical Journal of the Royal Astronomical Society 66, 157–168.
Hirata, N., Kinoshita, H., Katao, H., Baba, H., Kaiho, Y., Koresawa, S., Ono, Y., Hayashi, K., 1990. Report on DELP 1988 Cruises in the southern Okinawa Trough, part III: crustal structure of the southern Okinawa Trough. Bulletin of Earthquakee Res. Insti., Univ. Tokyo 66, 37–70.
Hourigan, J.K., Brandon, M.T., Soloviev, A.V., Kirmasov, A.B., Garver, J.I., Stevenson, J., Reiners, P.W., 2009. Eocene arc–continent collision and crustal consolidation in Kamchatka, Russian Far East. American Journal of Science 309, 333–396. http://dx.doi.org/10.2475/05.2009.01.
Hujita, K., 1980. The role of the Median Tectonic Line in the Quaternary tectonics of the Japanese Islands. Memoir — Geological Society of Japan 18, 129–153.
Igarashi, T., Iidaka, T., Miyabayashi, S., 2011. Crustal structure in the Japanese Islands inferred from receiver function analysis. Zisin 63, 139–151 (in Japanese with English abstract).
Iidaka, T., Takeda, T., Kurashimo, E., Kawamura, T., Kaneda, Y., Iwasaki, T., 2004. Configuration of subducting Philippine Sea plate and crustal structure in the central Japan region. Tectonophysics 338, 7–20. http://dx.doi.org/10.1016/j.tecto.2004.07.002.
Iidaka, T., Iwasaki, T., Yoshimoto, K., 2006. Non-transparent uppermost mantle in the island-arc region of Japan. Tectonophysics 420, 189–204.
Ikami, A., Ito, K., Sasaki, Y., Asano, S., 1982. Crustal structure in the profile across Shikoku, Japan as derived from the off Sakaide explosions in March, 1975. Zisin 35, 367–375 (in Japanese with English abstract).
Ishida, M., 1992. Geometry and relative motion of the Philippine Sea Plate and Pacific Plate beneath the Kanto–Tokai district, Japan. Journal of Geophysical Research 97, 489–513.
Isozaki, Y., Maruyama, S., 1991. Studies on orogeny based on plate tectonics in Japan and new geotectonic subdivision of Japanese islands. Journal of Geology 100, 697–761 (in Japanese with English abstract).
Ito, K., 1993. Cut-off depth of seismicity and large earthquakes near active volcanoes in Japan. Tectonophysics 217, 11–21.
Ito, K., 1999. Seismogenic layer, reflective lower crust, surface heat flow and large inland earthquakes. Tectonophysics 306, 423–433.
Ito, K., Yoshii, T., Asano, S., Sasaki, Y., Ikami, A., 1982. Crustal structure of Shikoku, southwestern Japan as derived from seismic observations of the Iejima and the Torigatayama explosions. Zisin 35, 377–391 (in Japanese with English abstract).
Ito, A., Hino, R., Nishino, M., Fujimoto, H., Miura, S., Kodaira, S., Hasemi, A., 2002. Deep crustal structure of the Northeastern Japan Forearc by seismic exploration using an air-gun array. Zisin 54, 507–520 (in Japanese with English abstract).
Ito, T., Kojima, Y., Kodaira, S., Sato, H., Kaneda, Y., Iwasaki, T., Kurashimo, E., Tsumura, N., Fujiwara, A., Miyauchi, T., Hirata, N., Harder, S., Miller, K., Murata, A., Yamakita, S., Onishi, M., Abe, S., Sato, T., Ikawa, T., 2009. Crustal structure of southwest Japan, revealed by the integrated seismic experiment Southwest Japan 2002. Tectonophysics 472, 124–134.
Iwasaki, T., Sato, H., 2009. Crust and upper-mantle structure of island arc being elucidated from seismic profiling with controlled sources in Japan. Zisin 61, S165–S176.
Iwasaki, T., Hirata, N., Kanazawa, T., Melles, J., Suyehiro, K., Urabe, T., Moller, L., Makris, J., Shimamura, H., 1990. Crustal and upper mantle structure in the Ryukyu Island Arc deduced from deep seismic sounding. Geophysical Journal International 102, 631–651.
Iwasaki, T., Yoshii, T., Moriya, T., Kobayashi, A., Nishiwaki, M., Tsutsui, T., Iidaka, T., Ikami, A., Masuda, T., 1994. Precise P and S wave velocity structures in the Kitakami massif, northern Honshu, Japan, from a seismic refraction experiment. Journal of Geophysical Research 99, 22187–22204.
Iwasaki, T., Kato, W., Moriya, T., Hasemi, A., Umino, N., Okada, T., Miyashita, K., Mizogami, T., Takeda, T., Seikine, S., Matsushima, T., Tashiro, K., Miyamachi, H., 2001. Extensional structure in northern Honshu arc as inferred from seismic refraction/wide-angle reflection profiling. Geophysical Research Letters 28, 2329–2332.
Iwasaki, T., Yoshii, T., Ito, T., Sato, T., Hirata, N., 2002. Seismological features of island arc crust as inferred from recent seismic expeditions in Japan. Tectonophyics 355, 53–66.
Iwasaki, T., Adachi, K., Moriya, T., Miyamachi, H., Matsushima, T., Miyashita, K., Takeda, T., Taira, T., Yamada, T., Ohtake, K., 2004. Upper and middle crustal deformation of an arc–arc collision across Hokkaido, Japan, inferred from seismic refraction/wide-angle reflection experiments. Tectonophysics 388, 59–73.
Kamiya, S., Kobayashi, Y., 2000. Seismological evidence for the existence of serpentinized wedge mantle. Geophysical Research Letters 27, 819–822.
Kato, A., Iidaka, T., Ikuta, R., Yoshida, Y., Katsumata, K., Iwasaki, T., Sakai, S., Thurber, C., Tsumura, N., Yamaoka, K., Watanabe, T., Kunitiomo, T., Yamazaki, F., Okubo, M., Suzuki, S., Hirata, N., 2010. Variation of fluid pressure within the subducting oceanic crust and slow earthquake. Geophysical Research Letters 37, L14310. http://dx.doi.org/10.1029/2010GL043723.

Katsumata, A., 2010. Depth of Moho discontinuity beneath the Japanese islands estimated by traveltime analysis. Journal of Geophysical Research 115. http://dx.doi.org/10.1029/2008JB005864.
Kazuka, T., Kikuchi, S., Ito, T., 2002. Structure of the foreland fold-and-thrust belt, Hidaka Collision Zone, Hokkaido, Japan: re-processing and re-interpretation of the JNOC seismic reflection profiles 'Hidaka' (H91-2 and H91-3). Bulletin of the Earthquake Research Institute—University of Tokyo 77, 97–109.
Kita, S., Okada, T., Hasegawa, A., Nakajima, J., Matsuzawa, T., 2010. Existence of interplane earthquakes and neutral stress boundary between the upper and lower planes of double seismic zone beneath Tohoku and Hokkaido, northeastern Japan. Tectonophysics 496, 68–82. http://dx.doi.org/10.1016/j.tecto.2010.10.010.
Kodaira, S., Iwasaki, T., Urabe, T., Kanazawa, T., Egloff, F., Makris, J., Shimamura, H., 1996. Crustal structure across the middle Ryukyu trench obtained from ocean bottom seismographic data. Tectonophysics 263, 39–60.
Kodaira, S., Kurashimo, E., Park, J.-O., Takahashi, N., Nakanishi, A., Miura, S., Iwasaki, T., Hirata, N., Ito, K., Kaneda, Y., 2002. Structural factors controlling the rupture process of a megathrust earthquake at the Nankai trough seismogenic zone. Geophysical Journal International 149, 815–835.
Kodaira, S., Iidaka, T., Kato, A., Park, J.-O., Iwasaki, T., Kaneda, Y., 2004. High pore fluid pressure may cause silent slip in the Nankai trough. Science 304. http://dx.doi.org/10.1126/science.1096535.
Kodaira, S., Sato, T., Takahashi, N., Miura, S., Tamura, Y., Tatsumi, Y., Kaneda, Y., 2007. New seismological constraints on growth of continental crust in the Izu–Bonin intra-oceanic arc. Geology 35, 1031–1034. http://dx.doi.org/10.1130/G23901A1.
Konstantinovskaya, I., 2001. Arc–continent collision and subduction reversal in the Cenozoic evolution of the Northwest Pacific: an example from Kamchatka (NE Russia). In: Lallemand, S., Liu, C.-S., Angelier, J., Tsai, Y.B. (Eds.), Active Subduction and Collision in Southeast Asia (SEASIA. Tectonophysics, v. 333. Elsevier, Amsterdam, pp. 75–94. http://dx.doi.org/10.1016/S0040-1951(00)00268-7. 10 April.
Kurashimo, E., Tokunaga, M., Hirata, N., Iwasaki, T., Kodaira, S., Kaneda, Y., Ito, K., Nishida, R., Kimura, S., Ikawa, T., 2002. Geometry of the subducting Philippine Sea Plate and the crustal and upper mantle structure beneath Eastern Shikoku Island revealed by seismic refraction/wide-angle reflection profiling. Zisin 54, 489–505.
Kurashimo, E., Iwasaki, T., Iidaka, T., Kawamura, T., Moriya, T., Shibutani, T., Miyamachi, H., Sato, H., Miller, K., Harder, T., Ito, Y., Kaneda, Y., Onishi, M., 2004. Deep seismic structure beneath the southwestern Japan arc, revealed by seismic refraction/wide-angle reflection profiling. Abstr. 11th Int. Symp. Deep Seismic Profiling of the Continents and Their Margins, p. 67.
Lander, A.V., Shapiro, M.N., 2007. The origin of the modern Kamchatka Subduction Zone. In: Eichelberger, J., et al. (Ed.), Volcanism and Subduction: The Kamchatka Region. Geophys. Monogr. Ser., vol. 172. AGU, Washington, D.C., pp. 57–64. http://dx.doi.org/10.1029/172GM05.
Langston, C.A., 1981. Evidence for the subducting lithosphere under southern Vancouver Island and western Oregon from teleseismic P-Wave conversions. Journal of Geophysical Research 86, 3857–3866.
Letouzey, J., Kimura, M., 1985. Okinawa Trough genesis: structure and evolution of the back-arc basin developed in a continent. Marine and Petroleum Geology 2, 111–130.
Levin, V., Park, J., 1997. P–SH conversions in a flat-layered medium with anisotropy of arbitrary orientation. Geophysical Journal International 131, 253–266.
Levin, V., Park, J., Brandon, M.T., Lees, J., Peyton, V., Gordeev, E., Ozerov, A., 2002a. Crust and upper mantle of Kamchatka from teleseismic receiver functions. Tectonophysics 358, 233–265.
Levin, V., Shapiro, N., Park, J., Ritzwoller, M., 2002b. Seismic evidence for catastrophic slab loss beneath Kamchatka. Nature 418, 763–767.
Matsubara, M., Obara, K., Kasahara, K., 2008. Three-dimensional P- and S-wave velocity structure beneath the Japan Islands obtained from the high-density seismic stations by seismic tomography. Tectonophysics 454, 86–103. http://dx.doi.org/10.1016/j.tecto.2008.04.016.
Matsubara, M., Obara, K., Kasahara, K., 2009. High-Vp/Vs zone accompanying non-volcanic tremors and slow-slip events beneath southwestern Japan. Tectonophysics 472, 6–17. http://dx.doi.org/10.1016/j.tecto.2008.06.013.
Miura, S., Takahashi, N., Nakanishi, A., Tsuru, T., Kodaira, S., Kaneda, Y., 2005. Structural characteristics off Miyagi forearc region, the Japan Trench seismogenic zone, deduced from a wide-angle reflection and refraction study. Tectonophysics 407, 165–188. http://dx.doi.org/10.1016/j.tecto.2005.08.001.
Mogi, K., 1981. Earthquake prediction program in Japan. In: Simpson, D.W., Rechards, P.G. (Eds.), Earthquake Prediction. An International ReviewMaurice Ewing Series, vol. 4, pp. 635–666.
Nakahigashi, K., Shinohara, M., Suzuki, S., Hino, R., Shiobara, H., Takenaka, H., Nishino, M., Sato, T., Yoneshima, S., Kanazawa, T., 2004. Seismic structure of the crust and uppermost mantle in the incipient stage of back arc spreading — northernmost Okinawa Trough. Geophysical Research Letters 31, L02614. http://dx.doi.org/10.1029/2003GL018928.
Nakajima, J., Matsuzawa, T., Hasegawa, A., 2001. Three-dimensionasl structure of Vp, Vs and Vp/Vs beneath northeastern Japan: implications for arc magmatism and fluids. Journal of Geophysical Research 106, 21,843–21,857.
Nakajima, J., Matsuzawa, T., Hasegawa, A., 2002. Moho depth variation in the central part of northeastern Japan estimated from reflected and converted waves. Physics of the Earth and Planetary Interiors 130, 31–47.
Nakajima, J., Takei, Y., Hasegawa, A., 2005. Quantitative analysis of the inclined low-velocity zone in the mantle wedge of northeastern Japan: a systematic change of melt-filled pore shapes with depth and its implications for melt migration. Earth Planet. Science Letters 234, 59–70. http://dx.doi.org/10.1016/j.epsl.2005.02.033.
Nakamura, K., 1983. Possible nascent trench along the eastern Japan Sea as the convergent boubdary between Eurasian and North American Plates. Bulletin of the Earthquake Research Institute 58, 711–722 (in Japanese with English abstract).
Nikulin, A., Levin, V., Shuler, A., West, M., 2010. Anomalous seismic structure beneath the Klyuchevskoy Group, Kamchatka. Geophysical Research Letters 37, L14311.
Nikulin, A., Levin, V., Carr, M., Herzberg, C., West, M., 2012. Evidence for two upper mantle sources driving volcanism in Central Kamchatka. Earth and Planetary Science Letters 321–322, 14–19.
Nishisaka, H., Shinohara, M., Sato, T., Hino, R., Mochizuki, K., Kasahara, J., 1999. Crustal structure of the margin of the northeastern Japan Sea using ocean bottom seismographs and controlled sources. Chikyu Monday 27, 75–82 (in Japanese).
Nishisaka, H., Shinohara, M., Sato, T., Hino, R., Mochizuki, K., Kasahara, J., 2001. Crustal structure of the Yamato Basin and the margin of the northeastern Japan Sea using ocean bottom seismographs and controlled sources. Zisin 54, 365–379 (in Japanese with English abstract).
Nishizawa, A., Asada, A., 1999. Deep crustal structure off Akita, eastern margin of the Japan Sea, deduced from ocean bottom seismographic measurement. Tectonophysics 306, 199–216.
Ohtsu, H., 2011. Crustal structure beneath eastern Kyushu — Factor of crustal deformation in southern Kyushu, Master Thesis, Graduate School of Science, the University of Tokyo.
Okada, H., Suzuki, S., Moriya, T., Asano, S., 1973. Crustal structure in the profile across the southern part of Hokkaido, Japan, as derived from explosion seismic observation. Journal of Physical Earth 21, 329–354.
Okada, H., Asano, S., Yoshii, T., Ikami, A., Suzuki, S., Hasegawa, T., Yamamoto, K., Ito, K., Hamada, K., 1979. Regionality of the upper mantle around northeastern Japan as revealed by big explosions at sea, I. SEIHA-I explosion experiment. Journal of Physical Earth 27, S15–S32 (Suppl.).
Okada, Y., Kasahara, K., Hori, S., Obara, K., Sekiguchi, S., Fujiwara, H., Yamamoto, A., 2004. Recent progress of seismic observation networks in Japan — Hi-net, F-net, K-NET and KiK-net, research news. Earth Planets Space 56 xv–xxviii.
Okamura, Y., 1990. Geologic structure of the upper continental slope off Shikoku and Quaternary tectonic movement of the outer zone of southwest Japan. Journal of the Geological Society of Japan 96, 223–237.
Okano, K., Kimura, S., Konomi, T., Nakamura, M., 1985. The focal distribution in Shikoku and its surrounding regions. Zisin 38, 93–103.
Otofuji, Y., Matsuda, T., Nohda, S., 1985. Opening mode of the Japan Sea inferred from the paleomagnetism of the Japan Arc. Nature 317, 603–604.
Ozawa, S., Murakami, M., Kaizu, T., Tada, T., Sagiya, T., Hatanaka, Y., Yarai, H., Nishimura, T., 2002. Detection and monitoring of ongoing aseismic slip in the Tokai region, central Japan. Science 298, 1009–1012. http://dx.doi.org/10.1126/science.1076780.
Park, J.-O., Tokuyama, H., Shinohara, M., Suyehiro, K., Taira, A., 1998. Seismic record of tectonic evolution and backarc rifting in the southern Ryukyu island arc system. Tectonophysics 294, 21–42.
Park, J., Levin, V., Brandon, M.T., Lees, J.M., Peyton, V., Gordeev, E., Ozerov, A., 2002. A dangling slab, amplified arc volcanism, mantle flow and seismic anisotropy near the Kamchatka plate corner. In: Stein, Seth, Freymueller, Jeffrey (Eds.), Plate Boundary Zones. AGU Geodynamics Series, No. 30. AGU, Washington DC, pp. 295–324.
Phinney, R.A., 1964. Structure of the Earth's crust from spectral behavior of long-period body waves. Journal of Geophysical Research 69, 2997–3017.
Portnyagin, M., Hoernle, K., Avdeiko, G., Hauff, F., Werner, R., Bindeman, I., Uspensky, V., Garbe-Schonberg, D., 2005. Transition from arc to oceanic magmatism at the Kamchatka–Aleutian junction. Geology 33, 25–28.
Research Group for Explosion Seismology, 1966. Explosion seismological research in Japan. In: Steinhart, J.S., Jefferson, S.T. (Eds.), The Earth Beneath the Continents. Geophys. Monogr. Ser., vol. 10. AGU, Washington, D.C., pp. 334–348.
Research Group for Explosion Seismology, 1992. Explosion seismic observation in the Kitakami Region, Northern Honshu, Japan (Kuji–Ishinomaki Profile). Bulletin of the Earthquake Research Institute—University of Tokyo 67, 437–461 (in Japanese with English abstract).
Research Group for Explosion Seismology, 1995. Explosion seismic observation in the central to western part of Honshu, Japan. Fujihashi–Kamigori Profile., Japan. Bulletin of the Earthquake Research Institute—University of Tokyo 70, 9–31 (in Japanese with English abstract).
Sato, H., 1994. The relationship between late Cenozoic tectonic events and stress filed and basin development in northeast Japan. Journal of Geophysical Research 99, 22261–22274.
Sato, H., Amano, K., 1991. Relationship between tectonics, volcanism, sedimentation and basin development, Late Cenozoic, central part of Northern Honshu, Japan. Tectonophysics 74, 323–343.
Sato, H., Ikeda, Y., 1994. Where is a boundary between Eurasian and north American plates in northern Japan? Abstract of the 1994 Annual Meeting of Geological Society of America, A208.
Sato, T., Takahashi, N., Miura, S., Fujie, G., Kang, D.-H., Kodaira, S., Kaneda, Y., 2006a. Last stage of the Japan Sea back-arc opening deduced from the seismic velocity structure using wide-angle data. Geochemistry, Geophysics, Geosystems 7, Q06004. http://dx.doi.org/10.1029/2005GC001135.
Sato, T., Sato, To, Shinohara, M., Hino, R., Nishono, M., Kanazawa, T., 2006b. P-wave velocity structure of the margin of the southeastern Tsushima Basin in the Japan Sea using ocean bottom seismometers and airguns. Tectonophysics 412, 159–171.
Shapiro, M.N., 1995. The Upper Cretaceous Achaivayamian–Valaginian volcanic arc and kinematics of the North Pacifc plates. Geotectonics 29, 52–64.
Shapiro, N.M., Gorbatov, A.V., Gordeev, E., Dominguez, J., 2000. Average shear-velocity structure of the Kamchatka peninsula from the dispersion of surface waves. Earth Planets Space 52, 573–577.
Shiomi, K., Sato, H., Obara, K., Ohtake, M., 2004. Configuration of subducting Philippine Sea plate beneath southwest Japan revealed from receiver function analysis based

on the multivariate autoregressive model. Journal of Geophysical Research 109, B04308. http://dx.doi.org/10.1029/2003JB002774.
Shiomi, K., Obara, K., Sato, H., 2006. Moho depth variation beneath southwestern Japan revealed from the velocity structure based on receiver function inversion. Tectonophysics 420, 205–221.
Sibuet, J.-C., Letouzey, J., Barbier, F., Charvet, J., Foucher, J.-P., Hilde, T.W.C., Kimura, M., Ling-Yun, C., Marsset, B., Muller, C., Stephan, J.-F., 1987. Back arc extention in the Okinara Trough. Journal of Geophysical Research 92 (14,041–14,063).
Stein, S., Freymueller, J.T. (Eds.), 2002. Plate Boundary Zones Geodyn. Ser., vol. 30. AGU, Washington, D.C. http://dx.doi.org/10.1029/GD030 (425 pp.).
Stern, R.J., Fouch, M.J., Klemperer, S.L., 2003. An overview of the Izu–Bonin–Mariana subduction factory. In: Eiler, J. (Ed.), Inside the Subduction Factory. Geophys. Monogr. Ser., vol. 183. AGU, Washington, D.C., pp. 175–222.
Suyehiro, K., Takahashi, N., Ariie, Y., Yokoi, Y., Hino, R., Shinohara, M., Kanazawa, T., Hirata, N., Tokuyama, H., Taira, A., 1996. Continental crust, crustal underplating and low-Q upper mantle beneath an oceanic arc. Science 272, 390–392.
Syracuse, E.M., Abers, G.A., 2006. Global compilation of variations in slab depth beneath arc volcanoes and implications. Geochemistry, Geophysics, Geosystems 7, Q05017. http://dx.doi.org/10.1029/2005GC001045.
Takahashi, N., Kodaira, S., Tsuru, T., Park, J.O., Kaneda, Y., Kinoshita, H., Abe, S., Nishino, M., Hino, R., 2000. Detailed plate boundary structure off northeast Japan coast. Geophysical Research Letters 27, 1977–1980.
Takahashi, N., Kodaira, S., Tsuru, T., Park, J.-O., Kaneda, Y., Suyehiro, K., Kinoshita, H., Abe, S., Nishino, M., Hino, R., 2004. Seismic structure and seismogenesis off Sanriku region, northeastern Japan. Geophysical Journal International 159, 129–145.
Takahashi, N., Kodaira, S., Tatsumi, Y., Yamashita, M., Sato, T., Kaiho, Y., Miura, S., No, T., Takizawa, K., Kaneda, Y., 2009. Structural variations of arc crusts and rifted margins in the southern Izu–Ogasawara arc–back arc system. Geochemistry, Geophysics, Geosystems 10, Q09X08. http://dx.doi.org/10.1029/2008GC002146.
Takeda, T, 1997. Detailed crustal structure in Central Japan as revealed from reanalysis of wide-angle data, Master Thesis, Graduate School of Science, the University of Tokyo.
Takeda, T., 2001. Improved mapping method for deep crustal imaging — application to wide-angle reflection data, Ph.D. Thesis, Graduate School of Science, the University of Tokyo.
Utnasin, V.K., Balesta, S.T., Erlikh, E.N., Anosov, G.I., German, L.L., Shantser, A.Ye., 1975. Deep-seated construction of the structural zones of Kamchatka. Soviet Geology 2, 67–80 ((in Russian) (Translated version: V.K. Utnasin, S.T. Balesta, E.N. Erlikh, G.I. Anosov, L.L. German & A.Ye. Shantser, Deep-seated construction of the structural zones of Kamchatka, International Geology Review Volume 18, Issue 1, pp. 1–12, 1976)).
Vinnik, L.P., 1977. Detection of waves converted from P to SV in the mantle. Physics of the Earth and Planetary Interiors 15, 39–45.
Yamaguchi, M., Hirahara, K., Shibutani, T., 2003. High resolution receiver function imaging of the seismic velocity discontinuities in the crust and the uppermpst mantle beneath southwest Japan. Earth Planets Space 55, 59–64.
Yamakita, S., Otoh, S., 2000. Estimation of the amount of Late Cretaceous left-lateral strike-slip displacement along the Median Tectonic Line and its implications in the juxtaposition of some geologic belts of Southwest Japan. Association for the Geological Collaboration in Japan. Monograph 49, 93–104 (in Japanese with English abstr).
Yoshii, T., 1994. Crustal structure of the Japanese islands revealed by explosion seismic observations. Zisin 46, 479–491 (in Japanese with English abstract).
Yoshii, T., Asano, S., 1972. Time-term analysis of explosion seismic data. Journal of Physics Earth 20, 47–57.
Yoshii, T., Sasaki, Y., Tada, T., Okada, H., Asano, S., Muramatsu, I., Hashizume, M., Moriya, T., 1974. The third Kurayoshi explosion and crustal structure in the western part of Japan. Journal of Physical Earth 22, 109–121.
Yoshii, T., Okada, H., Asano, S., Ito, K., Hasegawa, T., Ikami, A., Moriya, T., Suzuki, S., Hamada, K., 1981. Regionality of the upper mantle around northeastern Japan as revealed by big explosions at sea. II. Seiha-2 and Seiha-3 experiment. Journal of Physical Earth 29, 201–220.
Zhao, D., Horiuchi, S., Hasegawa, A., 1990. 3-D seismic velocity structure of the crust and the uppermost mantle in the northeastern Japan arc. Tectonophysics 181, 135–149.
Zhao, D., Horiuchi, S., Hasegawa, A., 1992a. Seismic velocity structure of the crust beneath the Japanese Island. Tectonophysics 212, 289–301.
Zhao, D., Hasegawa, A., Horiuchi, S., 1992b. Tomographic imaging of P and S wave velocity structure beneath northeastern Japan. Journal of Geophysical Research 97 (19,909–19.928).
Zhao, D., Hasegawa, A., Kanamori, H., 1994. Deep structure of Japan subduction zone as derived from local, regional and teleseismic events. Journal of Geophysical Research 99, 22313–22329.
Zlobin, T.K., Gureev, R.G., Zlobina, L.M., 2005. Deep structure of the southwest Kamchatka investigated using converted body waves from earthquakes. Russian Journal of Pacific Geology 24, 14–24 (in Russian).